Exosome dynamics and changes in a selection of their microRNA cargo in response to an acute bout of eccentrically-biased exercise in healthy human volunteers

by

Mr Jason Lovett

Thesis presented in fulfilment of the requirements for the degree of

"Master of Science in Physiological Sciences" in the "Science Faculty" at

Stellenbosch University

Supervisor: **Professor Kathryn H. Myburgh**

Co-supervisor: **Dr Peter Durcan**

March 2017

Declaration

By submitting this thesis electronically, I declare that the entirety of the work contained therein is my own, original work, that I am the sole author thereof (save to the extent explicitly otherwise stated), that reproduction and publication thereof by Stellenbosch University will not infringe any third party rights and that I have not previously in its entirety or in part submitted it for obtaining any qualification.

March 2017

Abstract

Background: Extracellular vesicles (EVs) are nanoscale (30 to 1000 nm diameter) mediators of intercellular information transfer, shuttling diverse cargos including functional nucleic acids, proteins and lipids. EVs are released by all cell types, are stable in circulation and are thus capable of transferring information between distant tissues. It has been established that circulating EV profiles adapt to differing physiological and disease states. However, a paucity of information on this type of communication arising from skeletal muscle is apparent, especially in the context of exercise. This is despite multiple opinion reviews highlighting the importance of EVs and their cargo (particularly microRNA) as biomarkers of muscle myopathies/dystrophies/damage and even as ameliorators of chronic diseases associated with a sedentary lifestyle.

Aims: To determine whether circulating EVs, within the exosome size range, display size, number and cargo alterations in response to exercise-induced muscle damage (EIMD) from an acute bout of eccentrically-biased exercise. Specific cargo selected for analysis included: miR-1, 133a, 133b, 206 and 31.

Methods: Blood samples were drawn from 9 human volunteers at baseline (BL), 2 and 24 hours after acute, sequential plyometric jumping and downhill running bouts. Leg muscle pain was assessed on a scale from 1 to 10. Serum creatine kinase (CK) activity was quantified spectrophotometrically. Plasma exosomes were isolated using size exclusion columns and visualised with transmission electron microscopy (TEM). Quantitative and qualitative information on exosome protein was determined by micro-bicinchoninic acid assays and Coomassie-stained gel visualisation respectively. Exosome sizes and numbers were quantified by nanoparticle tracking analysis (NTA). Selected microRNA (miR) cargo was reverse transcribed, and quantified using qPCR with normalisation to an exogenous control (cel-miR-39).

Results: Perceived muscle pain and serum CK were elevated post-exercise, providing indirect evidence for EIMD. A simplified protocol for fast exosome visualisation using TEM was achieved, and revealed an abundance of exosomes of varying sizes. A concomitant abundance of exosomes was found using the more precise NTA technique (mean = 9 x 10^{10} exosomes/ml plasma). Mean exosome diameters were 127 ± 15 nm across all timepoints. No change in exosome size or number was seen over time. Similarly, no change in exosome total protein concentration was apparent between timepoints. Exosome enrichment of the skeletal muscle-specific miR-206 was detected in all but one participant. Neither miR-206, nor ubiquitous myomiRs-1, -133a and -133b changed across timepoints. However, exosome miR-31 decreased from BL to 24 hr post-exercise ($p < 0.05$). Grouping of participants according to increases (responders) or decreases (non-responders) in exosome number from BL to 24 hr post-exercise revealed that exosome miR-133b decreased between BL and 24 hr post-exercise ($p < 0.05$) in non-responders ($n = 6$), with no characteristic change present in responders.

Conclusion: A profuse number of exosomes is present in human plasma. NTA analysis revealed that size exclusion was an effective exosome isolation method. Following EIMD the number or sizes of circulating exosomes did not change. Rather, exosome cargo profiles changed. Decreased exosome miR-31 following EIMD suggests the specificity of the response, with differences in response noted between responders and non-responders.

Uittreksel

Agtergrond: Ekstrasellulêrevesikels (EVs) dien as vervoermiddels van biologiese vrag en groottes is op nanoskaalvlak (30 to 1000 nm deursnee). EVs word vrygestel deur alle seltipes en is stabiel in sirkulasie, wat hul gepas maak om informasie intersellulêr te vervoer in die vorm van funksionele nukleïensure, proteïene en lipiede. Dit is voorheen vasgestel dat sirkulerende EV profiele aanpas volgens veranderinge in gesonde of ongesonde fisiologiese toestande. Desnieteenstaande bestaan daar 'n gebrek aan inligting vir skeletspier geassosieerde EVs, veral in die konteks van oefening. Ongeag hiervan het verskeie opinie resensies die gebruik van EVs en hul vrag (veral mikroRNS) as biomerkers vir spier miopatie/distrofie/beserings beklemtoon, asook hul potensiaal as genesingsmediators vir die kroniese siektes van 'n onaktiewe lewenswyse.

Doelwitte: Om te bepaal of 'n verandering in die grootte, getal en vrag van sirkulerende EVs, binne die eksosoom grootte beperking, veroorsak word deur oefening-geïnduseerde spierskade (OGSS), teweeggebring deur 'n eksentries-bevooroordeelde oefeningsessie. Spesifieke vragte geselekteer vir ontleding sluit in: miR-1, 133a, 133b, 206 en 31.

Metodes: Bloedmonsters van 9 menslike vrywilligers was geneem by basislyn (BL), 2 en 24 ure na akute, opeenvolgende pleometriese spronge en afdraand hardloopsessies. Beenspier pyn was geasesseer (skaal van 1 tot 10). Serum kreatien kinase (KK) aktiwiteit was spektrofotometries gekwantifiseer. Plasma eksosome was geïsoleer deur gebruik te maak van grootte uitsluitings kolomme en gevisualiseer dmv transmissie elektron mikroskopie (TEM). Kwantitatiewe en kwalitatiewe informasie vir eksosoom proteïene was bepaal deur mikro-bisinkonienieksuur toetse en Coomassie-kleuring van kladde onderskeidelik. Eksosoom groottes en hoeveelhede was gekwantifiseer dmv nanopartikel opsporings analise (NOA). Die geselekteerde mikroRNS (miR) was agteruit getranskribeer en gekwantifiseer met kPCR. En data is genormaliseer deur eksogene kontrole (cel-miR-39).

Resultate: Waargenome spierpyn en serum KK was verhoog na oefening en dui op indirekte wyse na OGSS. 'n Vereenvoudigde protokol vir spoedige EV visualisering dmv TEM was opgestel, wat 'n oorvloed van EVs van verkeie groottes ontbloot het. 'n Gepaardgaande oorvloed van eksosome was gevind met gebruik van die akurate NOA tegniek (gemiddeld 9 x10^{10} eksosome/ml plasma). Gemene eksosoom deursnee was 127 ±15 nm vir alle tydintervalle. Geen verandering in eksosoom grootte profiel of getal was met die verloop van tyd waargeneem nie, asook nie in totale eksosoom proteïen konsentrasie nie. Eksosoom vermeerdering van die skeletspier-geassosieerde miR-206 was gevind vir 8 van die 9 vrywilligers. Die hoeveelheid miR-206 asook alomteenwoordige myomiRs-1, 133a en 133b het onveranderd gebly tussen tydintervalle. 'n Afname in eksosoom miR-31 was wel waargeneem vanaf BL tot 24 uur na-oefening ($p<0.05$). Groepering van deelnemers volgens toenames (reageerders) of afnames (nie-reageerders) in eksosoom hoeveelhede vanaf BL tot 24 uur na-oefening het aan die lig gebring dat eksosoom miR-133b verminder het tussen tydintervalle ($p<0.05$) slegs in nie-reageerders (n=6).

Afsluiting: 'n Oorvloed van eksosome is teenwoordig in menslike plasma. NOA analise beaam dat grootte uitsluiting 'n effektiewe eksosoom ontginningsmetode was. Na afloop van OGSS het die profiel van die eksosoom vrag gedeeltelik verander, alhoewel die getal en grootte van sirkulerende eksosome onveranderd gebly het. 'n Vermindering slegs in eksosoom miR-31 na OGSS beklemtoom spesifisiteit. Verskillende reaksies is tussen reageerders en nie-reageerders waargeneem.

Acknowledgements

Firstly, I would like to thank my supervisor, Prof Kathy Myburgh. I thank you for your unconditional encouragement and support throughout a challenging and new area of research. Your insight into the scientific method, and ease at which you approach challenging information has helped me approach problems that I would not otherwise have considered. You always have an open door and a smile, allowing any urgent or stressful situations to be resolved quickly.

To my co-supervisor, Dr Peter Durcan, I greatly appreciate your constant troubleshooting advice. I thank you for the intriguing discussions on new, cutting-edge techniques and methods. The microRNA analysis in this thesis would not have been possible without your knowledge of RNA.

I would also like to thank Mr Ashwin Isaacs, who was available to draw blood at a minute's notice. Your calm and professional demeanor helped streamline the 27 blood draws in this study.

I would like to thank the National Research Foundation for their financial support throughout my MSc.

Lastly, I would like to thank my wonderful mother for her constant support throughout my education, and life in general. Thank you for convincing me that life is boundless, and that anything can be achieved. None of this would have been possible without your love and inspiration.

Table of contents

List of tables and figures

List of acronyms and abbreviations

AB	- Apoptotic body
ALIX	- ALG-2 interacting protein X
CAM	- Cell adhesion molecules
CD	- Cluster of differentiation
cDNA	- Complementary DNA
cel	- C. Elegans
CK	- Creatine kinase
Ct	- Cycle threshold
dH2O	- Distilled water
DHR	- Downhill running
DMD	- Duchenne muscular dystrophy
DOMS	- Delayed onset muscle soreness
EDTA	- Ethylenediaminetetraacetic acid
EIMD	- Exercise-induced muscle damage
ER	- Endoplasmic reticulum
ESCRT	- Endosomal sorting
EV	- Extracellular vesicle
Exo	- Exosome
FACS	- Fluorescence-activated cell sorting
HDL	- High-density lipoproteins
HELA	- Henrietta Lacks cells
HGF	- Hepatocyte growth factor
HGS	- HGF-regulated tyrosine kinase substrate
HnRNP	- Heterogenous ribonucleoprotein particle
HSP70	- Heat shock protein 70
HUVEC	- Human umbilical vein endothelial cells
IL-6	- Interleukin 6
ILV	- Intraluminal vesicles
ISEV	- International society for extracellular vesicles
LBPA	- Lysobisphosphatidic acid
LDL	- Low-density lipoprotein
miR	- microRNA
MRF	- Myogenic regulatory factors
MRF4	- Myogenic regulatory factor 4
Mrna	- Messenger RNA
MSC	- Mesenchymal stem cell
MV	- Microvesicle
MVB	- Multivesicular body
Myf5	- Myogenic factor 5
MyoD1	- Myogenic differentiation factor 1
MyoG	- Myogenin
MyomiR	- Muscle microRNA
Oct4	- Octamer-binding transcription factor 4
NSC-34	- Neuroblastoma spinal cord cell line 34
NTA	- Nanoparticle tracking analysis
PAGE	- Polyacrylamide gel electrophoresis
Pax 7 & 3	- Paired box transcription factor 7 & 3
PBS	- Phosphate-buffered saline
PCR	- Polymerase chain reaction
PHM	- Primary human myoblasts
PMJ	- Plyometric jumping
PMP	- Perceived muscle pain
qRT-PCR	- Quantitative Real-time PCR
RNA	- Ribonucleic acid

ROS	- Reactive oxygen species
rRNA	- Ribosomal RNA
SC	- Satellite cell
SDS	- Sodium dodecyl sulfate
SEC	- Size exclusion column
SkM	- Skeletal muscle
STAM	- Signal transducing adaptor molecule
TEM	- Transmission electron microscopy
tRNA	- Transfer RNA
TSG101	- Tumour suppressor gene 101

Chapter 1: Skeletal muscle

1.1 Introduction

Skeletal muscle (SkM) is a large tissue that constitutes approximately 40% of lean body mass in humans. SkM is at the center of numerous physiological processes eg. the expenditure of ATP to maintain core body temperature, force production for movement and the storage of proteins, fats and carbohydrates (i.e. structural proteins, triglycerides and glycogen, respectively). SkM is constantly required to synchronise local and systemic communication to maintain homeostasis and the ability to perform efficient work. This is not only necessary in healthy individuals, but also in circumstances where individuals rely on muscle breakdown as a source of energy (eg. cachexic patients), or those needing to compensate for decreased functional capacity due to muscle wasting (eg. in the condition known as sarcopenia).

Myopathies and dystrophies are degenerative conditions of SkM that can either be inherited or acquired, and result in a significantly decreased capacity for muscular work [1]. At present, limited treatment strategies are available for Duchenne muscular dystrophy, cachexia and sarcopenia patients. This is despite muscle damage having been of concern to researchers since the 1950's, when 14 studies were published (PubMed search terms: "muscle damage" NOT "cardiac" NOT "heart") on such diverse forms as; ischemic damage resulting from battlefield injuries [2], workplace nerve injuries leading to atrophy [3] and muscle complications of hemophilia [4].

SkM injuries in amateur and professional sport are also a routine occurrence, whether in training or competition. A detailed understanding of molecular and cellular events that occur during muscle injury and repair is essential to the development of intervention strategies that can enhance efficiency of regeneration and reduce recovery times. Such improved understanding will also aid in the development of strategies to delay muscle disease progression. The importance of SkM research becomes evident when one considers that the decade between 2006 and 2015 yielded 7728 publications on muscle damage (using the same

search terms listed above). The vast number of new publications per year is indicative of new information on muscle damage continuously being uncovered. It is not within the scope of this thesis to review all this research comprehensively. Instead, this literature review will start with an introductory overview of key processes/issues in skeletal muscle damage (Chapter 1), and then proceed to a more detailed review of extracellular vesicles (Chapter 2), key studies involving extracellular vesicles, and the position of skeletal muscle research in this emerging field (Chapter 3).

1.2 A brief overview of skeletal muscle structure

Skeletal muscle is connected to bone by integrated, tough and fibrous tendons. Muscle contractions cause a pull on tendons that results in movement of the connected bone. Whole skeletal muscle is comprised of abundant myofibres held together in bundles by perimysium connective tissue (Figure 1.1). The perimysium is surrounded by the epimysium which connects to the strong myotendinous junction. This network of connective tissue is not only necessary for force to be transferred to the bones, but also provides resilience and protection from stretch-induced damage. Muscle is supplied by large blood vessels embedded in the perimysium (Figure 1.1). Considering the myofibres themselves, each is multinucleated and surrounded by a sarcolemma. A vast network of capillaries is intimately linked to the myofibre bundles, so that oxygen, nutrients and other biological molecules (e.g. hormones, cytokines, growth factors) can reach each myofibre readily. Similarly, the capillary network has a venous side, removing products of muscle metabolism and other factors (examples of which will be discussed in the forthcoming sections of this, and the next chapter).

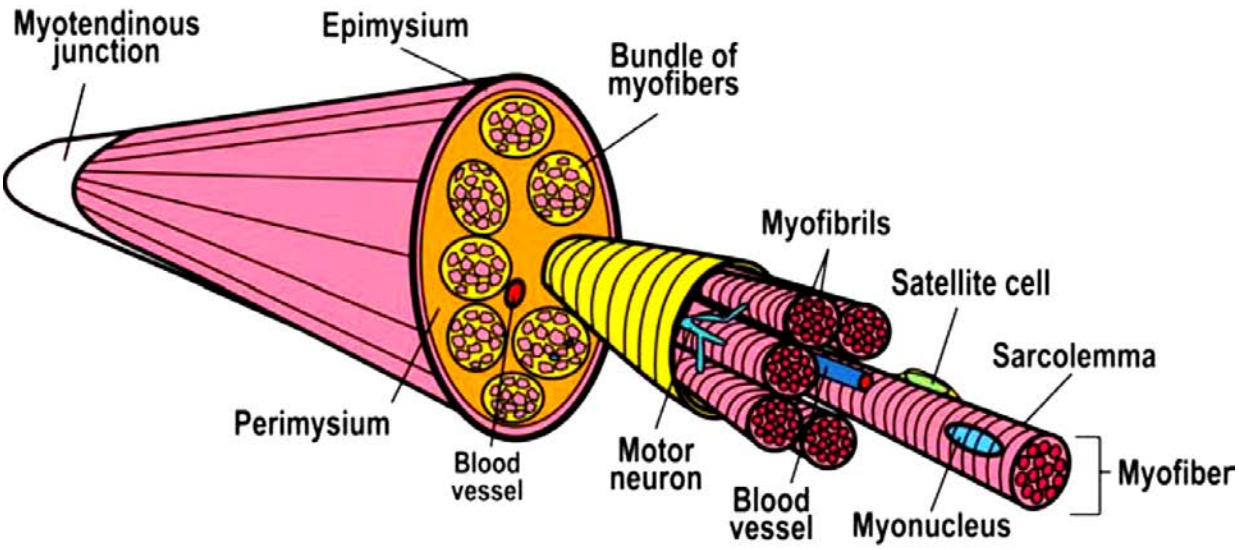

Figure 1.1. Brief overview of whole skeletal muscle structure. Figure from *Scime et al* with permission [5].

1.3. Introduction to skeletal muscle damage and regeneration

Sarcomeres, the functional unit of SkM, are responsible for tension development and the resultant contraction of the myofibre. Contraction of multiple myofibers is synchronised across the muscle to allow for sufficient tension. At the molecular level, sarcomeres are shortened through the action of myosin heads pulling on actin chains. To allow for significant force development, these two contractile proteins are sturdily held in place by Z-lines. Z-lines, in turn, are linked together by the abundant myoprotein, desmin. The large, elastic protein, titin, connects myosin tails to Z-lines, and allows the sarcomere to readily return to a resting position following contraction. However, contraction at the sarcomere level is not always synchronised and individual sarcomeres can become damaged during normal contraction. It is in fact its role in tension development that makes SkM a common site for injury. A theory of "popping sarcomeres" has been described in detail by *D. Morgan* in 1990 [6]. In this theory, weaker sarcomeres "pop" when muscle is stretched beyond it's normal length-tension relationship i.e. when myosin heads no longer overlap with actin chains. Some types of contraction make it more likely for such damage to occur (see *Morgan and Proske, 2004* [7]).

The diversity of SkM injuries in humans ranges from damage of weaker sarcomeres to traumatic tears of the whole muscle. Although the magnitude of injury may differ substantially, all require a highly effective regenerative response. Indeed, SkM exhibits great regenerative capacity, largely owing to a resident pool of myoblast progenitor cells, known as satellite cells (SCs) [8]. However, SCs do not operate as an independent entity. At the heart of SkM regeneration is a symphony of endocrine and paracrine signaling involved in local and widespread biological communication. Broadly, regeneration of SkM can be grouped into phases of inflammation, proliferation and differentiation, each with particular aspects of communication predominating [9].

1.3.1 Inflammation

Following damage, a complex secretome of cytokines and chemokines (i.e. collectively termed, myokines) is released by SkM into circulation. This systemic communication attracts pro-inflammatory immune cells to the damaged area. Neutrophils are some of the first circulating cells to infiltrate, releasing pro-inflammatory factors that create a positive feedback loop for the attraction of more immune cells [10]. During this initial inflammatory stage, neutrophils release proteolytic enzymes, such as matrix metallo-proteases and myeloperoxidase, and reactive oxygen species to degrade the damaged tissue and allow for complete destruction of the damaged area [11]. This can be visualised as a loss of ultrastructural organization (i.e. a lack of striated appearance in the damaged area, and Z-line streaming) [12]. Macrophages, displaying an M1 phenotype (i.e. pro-inflammatory), are next to infiltrate the area during overlapping phases of muscle destruction and phagocytosis of the resultant cellular debris [9]. The pro-inflammatory cytokine, IL-6, is one of the most abundant circulating cytokines following muscle injury [13]. The known responsiveness of macrophages to IL-6 signaling is an example of the organised and sequential immune response to molecular communication arising from muscle damage [14].

1.3.2 Proliferation

Following destruction and removal of debris, SC proliferation allows for the replacement of lost muscle cells and the restoration of fibre integrity if the damage is not severe enough for the entire fibre to be destroyed. These progenitor cells exhibit vast proliferative potential, and are

responsible for the high regenerative plasticity of SkM [15]. SCs are uniquely positioned on the inside of the basal lamina, and on the outside of the sarcolemma [8]. Their location allows for sensitive receival of both local and systemic communication. Hepatocyte growth factor (HGF), through resultant intracellular signaling after binding to c-met receptors, is a known activator of SCs. HGF is released by numerous cell types in the early phases of injury and degeneration, aiding SC activation.

The intricate control of proliferation and differentiation in myogenesis is largely achieved by a group of transcription factors, known as Myogenic regulatory factor (MRFs). This group includes; Myogenic differentiation factor 1 (MyoD), Myogenic factor 5 (Myf5), Myogenin (MyoG) and Myogenic factor 6 (MRF4) (Figure 1.2). MRFs are known to interact with a plethora of local and systemic signals (i.e. growth factors, microRNAs, cytokines). Two of the MRFs, MyoD and Myf5, are key during proliferation. MyoD is considered a "master regulator" of myogenesis due to its influence in cellular commitment to a myogenic profile. This role of MyoD is substantiated by its ability to commit cells with or without a mesodermal lineage, to a myogenic phenotype [16]. MyoD levels are increased following SC activation, and remain integral until the completion of differentiation. Myf5 is of most importance in maintaining the SC pool by designating some proliferating SCs to return to quiescence. Myf5 expression decreases as myogenesis progresses [17].

1.3.3 Differentiation

The differentiation/remodeling phase of regeneration is of most importance in determining the future function of the tissue. Insufficient structural reorganization of the regenerating area can result in a less efficient and less effective fibre. As a tissue recruited for work, SkM is reliant on an efficient and sturdy structure. The great capacity of SkM remodeling is largely responsible for this tissue's advanced regenerative plasticity.

During the remodeling phase *in vivo*, Macrophages displaying an M2 phenotype (i.e. regenerative) predominate [9]. Within new myoblasts, derived from SC proliferation, MyoG and MRF4 are of most important during this phase. Myogenin (MyoG) levels substantially increase during differentiation [18]. MyoG is key in transcribing factors associated with proliferation

inhibition (i.e. cyclin-inhibiting proteins), and allows for myoblast differentiation. MRF4, or herculin, is also upregulated during differentiation, and is key in myoblast fusion and myofibre maturation [19].

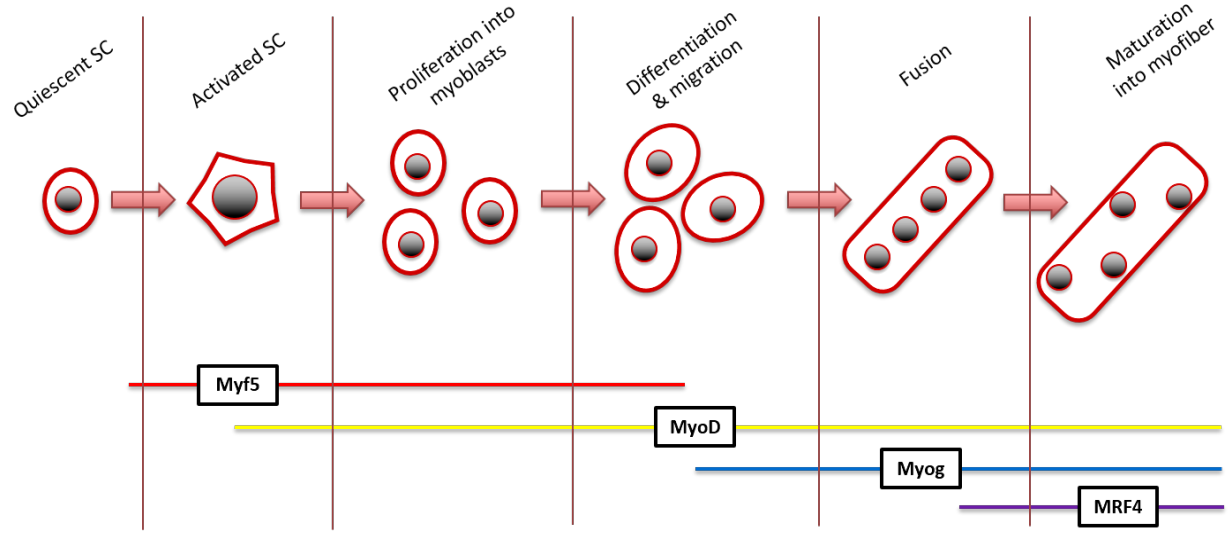

Figure 1.2. Schematic of satellite cell activation, proliferation and differentiation, with the corresponding myogenic regulatory factors involved.

1.4 Exercise induced skeletal muscle damage

Immediately following traumatic SkM injury, pain and swelling help to immobilise the injured area. In a milder and more diffuse damage, such as that seen with exercise-induced muscle damage (EIMD), range of motion is limited by tenderness experienced with movement. The lack of movement allows for regeneration to be prioritised over contractions.

Many models of SkM regeneration have been developed using animal studies eg. crush injuries [20] and cardiotoxin-induced muscle damage [21]. However, most cannot ethically be upscaled to human models. It is possible to analyse regeneration in the context of naturally occurring human muscle injury (eg. in sport or work-related injuries), but this is logistically very unpredictable and a consistent injury cannot be expected. Similarly, myopathies may be harnessed to analyse regeneration. However, an afflicted tissue is used, and the chronic nature

of this affliction does not mimic acute injury. One method that does allow for the analysis of the full spectra of moderate muscle damage in heathy human subjects *in vivo* is exercise-induced muscle damage (EIMD). SkM is an important tissue for *in vivo* research in its ability to be voluntarily recruited for work, a characteristic distinguishing it from smooth muscle. It can therefore be manually manipulated through exercise, allowing experimentation within the context of normal physiology.

Three types of muscle contractions exist; isometric, concentric and eccentric. These manifest as no change in muscle length, muscle shortening and muscle lengthening, respectively. Eccentric contractions add significantly more strain to a muscle than the concentric contractions that predominate daily activity [22]. This is a result of the fewer motor units recruited, intensifying the strain on each fibre. Muscle damage from unaccustomed or excessive eccentric contractions in laboratory protocols manifests much like the classic delayed onset muscle soreness (DOMS) sometimes experienced 24-48 hours after somewhat intense eccentrically-biased exercise undertaken in daily life (eg. walking down a flight of stairs, or slowly putting down a heavy object). The extent of damage can then be assessed by a combination of strategies. Direct assessment involves muscle biopsy and visualisation of sarcomere ultrastructure changes with microscopy [23]. Indirect assessment of muscle damage includes assessment of perceived muscle soreness [10] and the analysis of isometric force output [22]. Eccentric exercise protocols, such as downhill running and plyometric jumping, have been shown to successfully induce transient muscle damage in humans [10 12 13 24].

Of importance for this thesis is the ample evidence that eccentrically-biased protocols cause changes in circulating damage and inflammatory markers (typically creatine kinase and interleukin-6, respectively) [14 25]. However, changes in these markers are variable and do not reflect the extent of damage, but simply that EIMD has occurred. The identification of alternate circulating biomarkers of EIMD have been pursued, particularly involving the cytokine families eg. Il-8 [26] and IL-10 [27]. However, these markers originate from injured muscle cells, uninjured exercising muscle and immune cells [28]. Therefore, there are still no stringently validated biomarkers of skeletal muscle damage, and new options are continuously being sought.,

particularly amongst circulating factors that are easily accessible by blood sampling (for a recent review see *Rebalka and Hawke, 2014* [29]).

Chapter 2: Extracellular vesicles

2.1 Introduction to extracellular vesicles

Over the past decade, a novel form of intercellular communication has emerged: Extracellular vesicles (EVs) are nano-scale, stable and selective mediators of cellular information transfer [30]. They are comprised of a spherical, cell-like lipid bilayer that affords the protection of the macromolecules that are their cargo (i.e. lipids, proteins and nucleotides). They are found in biofluids such as blood, urine and saliva [31]. EVs are categorised into small 30-150 nm (exosomes), medium 100-1000 nm (microvesicles), and large 1 μm and greater (most typically apoptotic bodies), and have been found to be secreted by almost all cell types [30]. Apoptotic bodies are important mediators of cell death. In contrast, exosomes and microvesicles deliver cargo between cells and therefore may play a more functional role [32] [33] [34]. In much of the peer-reviewed literature, exosomes and microvesicles are collectively termed exosomes. However, it is more correct to use the term vesicles, in particular, "extracellular vesicles (EVs)" in accordance with guidelines set by the International Society of Extracellular Vesicles (ISEV) [35].

2.2 The emergence of EV biology

The presence of EVs was first established in blood research, by *Chargaff and West* in 1946 [36]. In trying to better understand the mechanisms of blood clotting, these researchers noted a protein pellet in human plasma following high speed centrifugation (i.e. 31 000 g). When supplemented onto plasma taken from a patient with hemophilia (i.e. blood void of clotting factors), blood coagulation was noted. In 1967, *Peter Wolf* made use of transmission electron microscopy to visualise intact particles in similar plasma pellets [37]. He termed these spherical particles, "platelet dust", but did not identify their vesicular nature. Just over two decades later, *Pan et al* monitored the fate of immuno-gold labelled transferrin receptors during experiments aimed at elucidating the maturation of reticulocytes [38]. At that time, it was known that transferrin receptors were only present in immature reticulocytes. These researchers noted "selective externalisation of the antibody-receptor complex", and concluded that the necessary extrusion

of the receptor during reticulocyte maturation was facilitated by vesicle secretion. "Platelet dust" was then retrospectively also seen to be vesicular in nature. Together, these studies established the presence of vesicles in blood, some of which at least were also functional.

In a pioneering study by *Raposo et al*, EVs were revealed to confer antigen-presenting information between immune cells *in vitro* [39]. These researchers supplemented EVs derived from antigen-exposed B cells onto T-cells, and recognised the mediation of antigen information through MHC class 2 integration into EVs. This study established the role of EVs in the transfer of immune competency between cell types, helping to establish their roles as functional mediators of intercellular communication. A decade later, *Ratajczak et al* noted the presence of mRNA transcripts in EVs [40]. Furthermore, this group found that some mRNA transcripts were enriched in EVs when compared to their expression levels in parent cells. However, it was not until a pivotal study by *Valadi et al* a year later, that EV biology really began to emerge [41]. Using radio-labelled nucleotides, this Swedish research group showed that EVs not only encapsulate RNA, but deliver RNA species between cells. Astoundingly, this transferred RNA remained functional, and was transcribed in the recipient cell. These findings have greatly propagated research into EV biology.

2.3 EV biogenesis, release and uptake

2.3.1 Biogenesis

Both types of EVs originate from the plasma membrane. Larger microvesicles (100-1000 nm) bud directly from the cell membrane in a blebbing-like process. Smaller exosomes (30-150 nm) form through endocytosis of the cell membrane into an early endosome. Maturation of this early endosome involves repeated steps of inward budding/pinocytosis, resulting in a multivesicular body (MVB) containing many intraluminal vesicles (ILVs) [42] (Figure 2.1). Upon stimulation, the membrane of MVBs fuse with the plasma membrane of the parent cell, and ILVs are released into the extracellular space. Once exocytosed, ILVs are then termed exosomes. A focus will be placed on exosome biogenesis in this thesis.

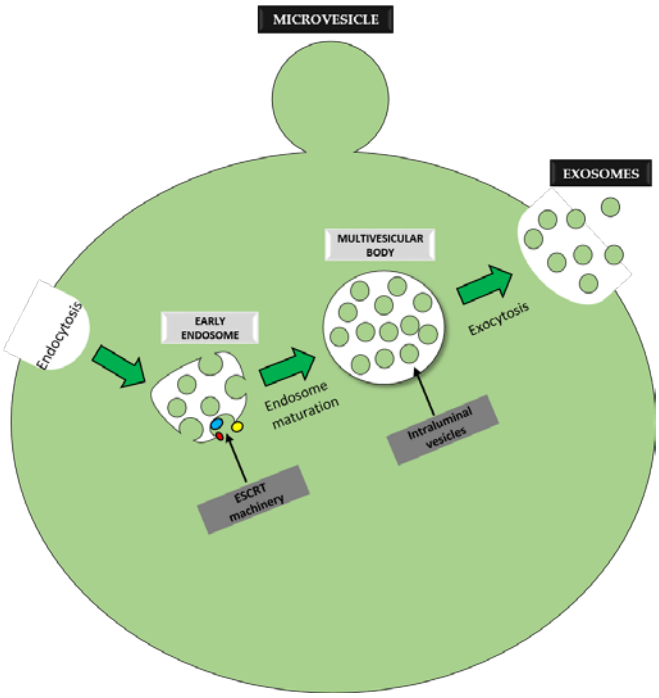

Figure 2.1. Diagram of extracellular vesicle biogenesis and release.

The best described pathway for exosome formation involves a family of ± 20 proteins, collectively termed the endosomal sorting complex required for transport (ESCRT) (Figure 2.1) [43]. The ESCRT family forms four complexes that, along with associated proteins, are widely considered key in the coordination of MVB formation and ILV packaging [43]. ESCRT-0 proteins incorporate ubiquitin-tagged membrane proteins into exosomes, through the actions of the proteins; HGS (hepatocyte growth factor-regulated tyrosine kinase substrate) and STAM (signal transducing adaptor molecule) [44]. ESCRT-1 & 2 are responsible for bud formation and cargo packaging of ILVs, occurring during maturation of an early endosome into a MVB. This process is aided by the commonly identified EV-enriched proteins; TSG101 (tumour suppressor gene 101) and ALIX (programmed cell death interacting protein 6) [43]. ESCRT-3 proteins are responsible for the excision of the bud, allowing for isolation of ILVs from the cytosol of the parent cell [43]. It is important to note that the exact mechanisms of cargo selection and recruitment to the ILVs are yet to be established. Given this, the ESCRT family cannot be taken as the complete description for exosome formation. For example, MVBs have been shown to form in the absence of some ESCRT proteins [45]. Non-ubiquitinated proteins have been shown to

be packaged into ILVs, suggesting that packaging may occur through unlabeled-protein, or non-ESCRT-0 related, mechanisms [46]. A candidate for directing cargo to ILVs is heat shock protein 70 (HSP70), an established protein chaperone in physiological processes like autophagy [47]. Interestingly, this protein is enriched in EVs and is now proposed as a vital mediator of selective cargo packaging into EVs [48] [49].

Taken together, these studies suggest that exosome biogenesis is complex. Although the key players in the synchronization of vesicle formation remain to be precisely elucidated, advances in EV analysis are piecing together the fragmented picture at a rapid rate.

2.3.2 Release

Studies using electron microscopy have captured sequences of images suggesting that exosome release into the extracellular space occurs through fusion of MVBs with the parent cell plasma membrane [39] [42]. Interestingly, not all MVBs are directed toward the plasma membrane. Distinct subpopulations are apparent. MVBs are either directed toward lysosomes for degradation, or to the plasma membrane for exocytosis of their ILVs. In reticulocytes, MVBs positive for Rab5, an early endosome marker, are directed to the plasma membrane [50]. Five additional members of the Rab family of proteins; Rab 2b, 5a, 9a, 27a and 27b have also been implicated in regulation of exosome release [51], thereby highlighting the important role of the Rab family in exosome release. In contrast, the presence of some classical endosomal proteins, such as LBPA, are known to direct MVBs toward lysosomes [48]. Therefore, the protein composition of MVBs appears to regulate their fate. The lipid content also seemingly plays a key role in MVB trafficking through the cytosol, as cholesterol-enriched MVBs preferentially fuse with the plasma membrane [52].

Although some biomolecular profiles, as mentioned above, have been correlated with exosome release, the stimuli for release are not well-established. The extent of exosome release *in vitro* has been reported to be affected by an array of different stimuli. For example, diverse molecules, such as calcium [53], potassium [54] and ATP [55] have been shown to affect the quantity of exosome release into media. These early studies show a small fraction of the diverse stimuli that

have since been shown to alter exosome release (for a recent review see *Colombo et al, 2014* [43]). However, much less is known about exosome uptake.

2.3.3 Uptake

Generally, EV uptake occurs through one of three mechanisms following a receptor-ligand type interaction. An EV can either fuse with the recipient cell membrane to release its cargo into the recipient cell [56], be engulfed (intact) and directed to cell compartments [57] [58], or potentially not release its cargo but behave more like a ligand resulting in a classic receptor-ligand intracellular signaling cascade [59].

Internalization of intact EVs has been described through the mechanisms of; polymerization-dependent phagocytosis by macrophages [60], receptor-mediated endocytosis [57] and lipid-raft dependent fusion [61] to name but a few. An example of EVs, or their cargo, not internalised by the recipient cell was shown in a study by *Denzer et al* [62]. These researchers isolated EVs from antigen-presenting cells, and noted that internalization was not necessary for transference of immune competency.

To better understand EV uptake and whether or not it is specific, *Alvarez-Erviti et al* engineered EVs to present a surface receptor containing an amino acid sequence that would be recognised by receptors specifically expressed on either neuronal or muscle cells [63]. The engineered EVs bound only to the cells of the neuron or muscle cell line, to which their surface receptor sequence had been targeted. This implies that EV uptake is most likely highly specific, at least some of the time.

2.4 EV Cargo

2.4.1 Lipids

EVs are comprised of a lipid bilayer, with the orientation resembling that of their parent cells. Regarding the structure and content of EVs, their lipid bilayer and possible lipid cargo have received the least attention to date (Figure 2.2). Nonetheless, differences between EV membranes and parent cell membranes is rapidly becoming apparent.

Cholesterol, phosphatidylserine and sphingomyelin have been found to be particularly abundant in EV membranes when compared to the plasma membrane from which they were derived [64]. Collectively, these lipids manifest in tightly-packed, organised, and lipid-dense regions of the EV membrane, known as lipid rafts [65]. The existence of lipid rafts on EV membranes is substantiated by the presence of the lipid raft-associated protein, flotillin-1 [66], which is also characterised as one of the EV-enriched proteins. Lipid rafts are widely considered essential to the stability of EVs within biofluids, as their constituent lipids are known to provide rigidity [66]. However, whether these lipid rafts are formed at the early endosome, or are endocytosed from the parent cell membrane, is yet to be established. However, as biomarkers, EV membrane profiles may emerge as important.

Recently, a difference in lipid profile between urine-derived EVs (healthy individuals) and cancer cell media-derived EVs has been shown [32], with cholesterol levels higher in the former. This further supports the hypothesis that circulating EVs display a lipid profile that allows for their stability within biofluids. The lipid profile of EVs has received significant attention from cancer researchers [32] [33]. Cancer cells likely exhibit a different lipid profile to aid their survival in hypoxic, elevated ROS and acidic environments. The release of EVs from damaged tissue may, therefore, likely also be different to basal EVs in circulation of healthy individuals.

Lipids are not only responsible for the structure of EVs, but can also play a role in communication between cells since EVs contain lipids intra-luminally. *Subra et al* showed the capacity for EVs to transfer a physiologically-relevant concentration of prostaglandins into the

cytosol of recipient cells i*n vitro* [67]. This study, like others, highlights the role of EVs as a functional unit of intercellular communication.

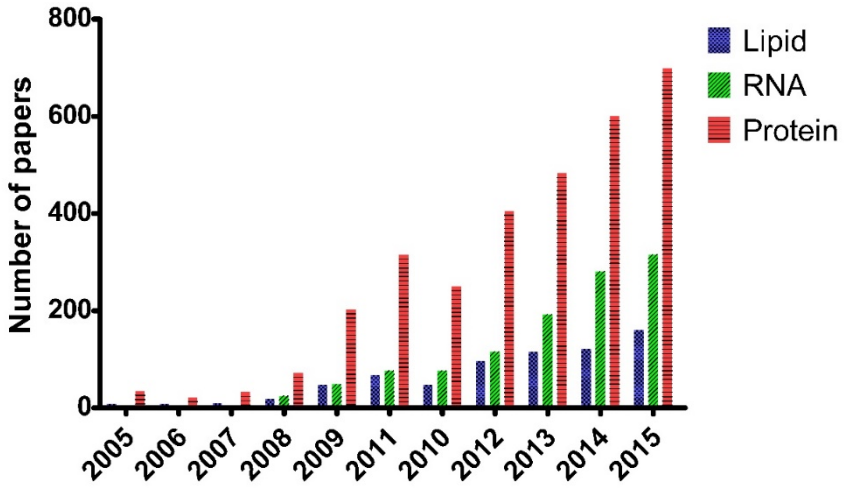

Figure 2.2. Number of published EV papers focusing on proteins, RNA or lipids as structural elements or cargo published from 2005-2015. Data was taken from PubMed, using an advanced search for "extracellular vesicles" OR "exosomes" OR "microvesicles" AND "protein"/ "RNA" or "lipid".

2.4.2 Protein

Proteins are not only part of the EV cargo, but also established components embedded in the lipid bilayer. Three members of the tetraspanin family of transmembrane proteins, CD9, CD63 and CD81, are some of the most commonly identified EV-enriched proteins, as per the online EV database, ExoCarta (ExoCarta.org). Not surprisingly, the ESCRT family proteins are also enriched in EV isolates. It is important to note that the abundance of EV-enriched proteins is altered between differing physiological conditions and cell/organism types [35], and a consistent profile has not been established. This may be why no definitive protein has been identified as an exclusive EV marker. Nonetheless, attempts have been made to promote ESCRT-associated proteins, i.e. TSG101 and Alix, as appropriate identifiers [35].

Advances in mass spectrometry have aided the identification of a vast number of proteins in EVs. A wide variety of proteins have been found eg. transcription factors, cytokines, receptors

and growth factors [48] [68] [69]. Furthermore, a diversity in the EV proteome is also apparent between cell types and physiological state. New online databases, such as; EVpedia (evpedia.info), ExoCarta (ExoCarta.org) and Vesiclepedia (microvesicles.org), have been established to sort and with more time to standardise the large amount of data currently being generated on EV proteins.

2.4.2.1 EV-enriched proteins are used for quality control of EV isolation

In 2014, ISEV has proposed a set of minimal experimental requirements to determine the existence of EVs in an isolate [70]. In this position paper, it was proposed that both positive and negative protein markers should be employed to ascertain the presence and purity of EVs. The presence of EVs should be established through the detection of at least two proposed protein groups (See Table 2.1).

The presence of EV-enriched membrane proteins (both transmembrane and membrane-associated) is required to define the correct isolation of EVs (Table 2.1 A & B). Characterization of EV-related proteins is convoluted by the frequent co-isolation of contaminating proteins (Table 2.1 D). The reason for this contamination is not well understood, but is hypothesised to result from molecules of similar density or aggregation mechanisms. Furthermore, given the physiologically relevant mediation of communication by EVs, as opposed to the random incorporation of cellular components in ABs during cell death, the presence of organelle structural proteins is used as a negative control.

A. EV-enriched transmembrane	B. EV-enriched membrane-associated	C. Not expected (of organelle origin)	D. Contaminating
Tetraspanins (CD9[1],63[7],81[24])	Alix[3]	ER (Calnexin)	Albumin
CAMs	TSG101[11]	Nuclear	HDL & LDL
Flotillin[41]	HSP70[2]	Golgi (organelle)	Immunoglobulins

Table 2.1. Four groups of proteins proposed by ISEV, to define the presence of EVs in an isolate. Top identified proteins are denoted by a superscript corresponding to their position on the top 100 most identified proteins list (ExoCarta v.3.2).

2.4.3 RNA

As mentioned before, the presence of EV RNAs was first discovered in 2006 [40]. In 2007, *Valadi et al* using microarray profiling of the RNAs and identified the presence of over 1300 different mRNAs, and 120 different microRNAs in EVs isolated from a mast cell line (MC/9). In the same paper these authors reported the mRNA and microRNA content in EVs in comparison to that of the parent cells and revealed an enrichment of particular RNAs in EVs. Furthermore, they reported the capacity of EVs to transfer RNA to recipient cells. This study raised so many intriguing questions that it is considered instrumental in the propagation of the EV research field (see consistent increase in EV RNA studies in Figure 2.2).

Messenger RNA (mRNA) forms the intermediate phase in the central understanding of molecular biology, whereby DNA is transcribed into RNA, which is subsequently translated into proteins. The transfer of mRNA in EVs provides a unique opportunity for protein to be translated in a separate cell/tissue from that in which it was initially transcribed. However, RNAs found in EVs are predominantly smaller than mRNA transcripts. Indeed, EVs are known to be enriched in microRNA and 3' untranslated region (UTR) mRNA fragments. Other small RNAs such as piwi-interacting RNA, tRNA, rRNA, yRNA and non-coding RNA have also been detected [71]. Of these, perhaps the most interesting is microRNA.

2.4.3.1 microRNA

microRNAs (miRs) are ± 22 nucleotide, single-stranded sequences responsible for post-transcriptional gene regulation. miRs are potent regulators of translation and hence have

downstream effects on many cellular functions. In humans, miRs exert their effects through the transient repression of messenger RNA (mRNA) translation. This is accomplished by incomplete binding of a miR to an mRNA transcript, preventing translation of the mRNA into protein. This incomplete binding chiefly occurs at the 3′ UTR of the mRNA [72], and allows miRs to target approximately 60% of the human genome. According to version 21 of miRBase (an online database for miRs run by the Sanger Institute), over 2500 human miRs have been identified. (See Appendix 1 for further detail on miR biogenesis and nomenclature).

From a functional point of view, it is now well known that one mRNA can be targeted by more than one miR, and it is possible for one miR to bind one mRNA at multiple sites. Furthermore, particular miRs can target multiple different mRNAs. This convolution of information has made the narrowing down of specific miR functions challenging, but in no way lessens their potential importance.

One might consider that the research fields of miRs and EVs are both still in their infancy, and the potential of both may allow these fields to progress in parallel. In the next chapter, key studies addressing the effects of EVs *in vitro*, as well as the origin of circulating EVs *in vivo* will be reviewed. Lastly, the next chapter will review the current understanding of EVs in the context of SkM.

Chapter 3: Key extracellular vesicle studies

3.1 Effects of EVs on cells

Specific cellular and physiological effects of EVs have been described in many fields. Perhaps the best described effects have been shown in the context of stem cell research. The supplementation of stem cell-derived EVs onto unipotent cell types, and vice versa, allowed researchers to gain an understanding of cell programming, reprogramming and dynamics that could become beneficial for regenerative medicine. Three examples of such studies will be presented below.

The supplementation of primary monocytes-derived EVs onto mesenchymal stem cells (MSCs) *in vitro* (i.e. two key cell types involved in tissue regeneration), has helped illuminate the role of EVs in deciding stem cell fate [73]. The researchers at the University of Gothenburg, Sweden showed that this EV addition propagated an osteogenic gene profile in MSCs. More specifically, they found the presence of osteogenic transcription factors in EVs, but not in the media suggesting that direct transfer was involved. *Sahoo et al* went a step further and found that CD34-derived EVs could enhance angiogenesis both *in vitro* in an endothelial cell culture and *in vivo* in mouse corneas [74]. In relation to skeletal muscle, a landmark study was done by *Hu et al* an *in vivo* mouse hind-limb ischemia/reperfusion model. The authors deduced that MSC-derived EVs perfused into the injury site lead to changes associated with enhanced healing, including increased blood flow to the injured area and an increase in the angiogenic molecular profile of the tissue. Possible mechanisms were elucidated *in vitro*, where increases in human umbilical-derived vascular endothelial cell (HUVEC) migration, proliferation and tube formation were found [75].

Such studies highlight the potent influences EVs can have at the cellular level as well as the potential of EVs as therapeutic agents. Their ability to carry cell/tissue-state specific information avoids critical fall-throughs encountered with other cell therapy modalities, such as the lack of

stem cell adherence to injured sites in stem cell injection studies and the seeming avoidance of an immune response in the recipient. Recently, the revelation of EV signatures that correlate to physiological states [33], has brought to light other promising applications of basic and applied EV research to the clinical setting.

3.2 Effect of physiology on EVs: state-specific and tissue-specific EVs

At present, a large proportion of EV research is directed toward identifying circulating EV profiles (i.e. of protein, RNAs or lipids), that may help negate the use of invasive tissue biopsies for diagnosis. The use of EVs as a less invasive "liquid biopsy", may facilitate early diagnosis of diseases if 'signatures' can be confirmed and may facilitate the monitoring of treatment interventions in a more sensitive and immediate manner.

Specifically, much current EV research is directed toward understanding tumour environments and tumour metastasis. Moreover, research into cancer diagnosis is now looking toward circulating EVs to determine the presence of cancers that would otherwise be too difficult to reach for biopsy. A recent revolution in EV biology saw a significant correlation between an EV-enriched membrane-associated protein, glypican-1 (GPC1), and pancreatic cancer in humans [33]. GPC1 increased in EVs isolated from patients' serum throughout the time course of tumour enlargement and stage development. These researchers found that this state-specific correlation was sensitive enough to discriminate between benign and cancerous tumors. In another recent study, *Skotland et al* made use of mass spectrometry to identify nine lipids from urinary EVs that showed significantly different expression between prostate cancer patients and healthy controls [32]. Additionally, 8 miRs (out of a selected panel of 43) were found to be decreased in $EpCAM^+$ (epithelial cell adhesion molecule) immuno-captured EVs derived from the plasma of patients with colorectal cancer [76].

However, the milieu of circulating EVs is very complicated. Some research groups have directed their attention towards the identification of tissue-specific markers on circulating EVs, attempting to delineate the tissue of origin of EVs. *Guescini et al* determined the existence of the

muscle-specific protein, alpha-sarcoglycan (SGCA), on the membrane of a portion of human plasma-derived EVs [34]. Using flow cytometry, they determined that 1-5 % of their sample was positive for SGCA, and that 60-65% of this subset was also positive for the EV-enriched protein, CD81. This study showed that more detailed profiling of tissue specific EV groups is possible and more research along these lines is likely in the future. The complexity of plasma-derived EVs may soon be simplified through compartmentalizing EVs harvested from the circulation by analysis of tissue of origin.

3.3 EVs and Skeletal muscle

Only a hand full of studies have investigated EVs in the context of SkM. Although the lesser number of these contribute to our current understanding of circulating EVs *in vivo*, the *in vitro* studies have contributed a great deal to the general method development in terms of EV isolation and analysis from blood. Here, these *in vitro* studies will be dealt with chronologically to illustrate the progression in EV analysis regarding SkM. For a direct comparison of details between the following 4 key studies, see Table 3.1.

The first identification of SkM cells releasing EVs occurred less than a decade ago in a study using the immortalised mouse myoblast cell line, C2C12s [77]. Highlights of this study included the comprehensive analysis of the EVs isolated from the media. This analysis included both positive identification of typical EV enriched proteins and visualisation using TEM. Of importance for theoretical aspects of muscle research was the identification of peptides and proteins, DNA and mitochondrial DNA that revealed the cargo contained some structural proteins, mitochondrial proteins, several heat shock proteins and even smaller proteins (i.e. low kDa) with the common characteristic of being able to influence cell signaling (e.g small GTP-binding protein, Rab7). In 2012, a relatively similar study was performed using primary human myoblasts (PHMs) [78]. This study used many of the same EV isolation techniques, but expanded on the first study mainly by separating the analysis of microvesicles and exosomes. Only 35% of the cargo was common to both types of vesicles. Eighteen % of the proteins identified were exclusively present in exosomes, whereas 47% were exclusively present in microvesicles.

Therefore, it became apparent that the consideration of vesicle size is of utmost importance in interpreting vesicle-mediated communication. Also, using a combination of proteomic and bioinformatic strategies, *Le Bihan et al* found that differentiating PHM-derived EVs contained a more diverse protein profile than expected. The presence of many proteins not considered to be involved in myogenesis led them to the hypothesis that myoblast-derived EVs may be important in intercellular communication between different cell types. Futhermore, two years later, *Forterre et al* elucidated large differences in EVs protein cargos when comparing myoblast states i.e. proliferating myoblast-derived EVs contained 31 proteins not found in myotube-derived EVs [79]. This suggested that EVs could also be important communicators during different stages of muscle damage and regeneration. Eventually, in that same year it was shown that EVs from differentiating C2C12 cells could aid neural cell survival and neurite outgrowth of the motor neuron cell line, NSC-34 [80]. This study was also the first to report the characterisation of SkM EVs using a technology called nanoparticle tracking analysis (NTA). This was significant as it allowed for the quantification of a heterogenous (according to size) pool of EVs based on size and number. This technology was to become important in future studies of EVs harvested from blood samples.

Author/ year	Model	EV isolation	EV analysis
***Guescini et al*, 2010** [77]	C2C12 (prolif)	24 hr DC + sucrose gradient	WB, TEM, MS & PCR
***Le Bihan et al*, 2012** [78]	PHM (diff)	24, 48 & 72 hr DC + iodixanol gradient	WB, TEM, MS, Luminex profiling, RNA microarray & CM
***Forterre et al*, 2014** [79]	C2C12 (diff)	48 hr DC	WB, TEM (+ gold), NanoSight, qRT-PCR, MS, transfection & FM
***Madison et al*, 2014** [80]	C2C12 (diff) & NSC-34 (diff)	48 & 96 hr DC	WB, NanoSight & FM,

Table 3.1. Chronological detailing of studies analysing EVs in the context of SkM *in vitro*. (PHM = primary human myoblasts, diff = differentiating, prolif = proliferating, DC = differential centrifugation, WB = western blotting, TEM = transmission electron microscopy, MS = mass spectrometry, FM = fluorescence microscopy, CM = confocal microscopy).

3.3.1 EVs and skeletal muscle regeneration

Briefly mentioned before, mesenchymal stem cells (MSCs) are multipotent cells with key roles in the regeneration of many tissue types. Recently, a comprehensive study on MSC-derived EVs and SkM regeneration was published by *Nakamura et al* [81]. These researchers elaborated on the paracrine effects of MSCs by showing that their EVs could promote myogenesis and angiogenesis in C2C12 and HUVEC cells, respectively. These same effects were confirmed on skeletal muscle *in vivo*, where EVs were injected into the site of injury in a mouse model of cardiotoxin-induced muscle injury. This study, alongside the previously mentioned study of *Hu et al* [75] on hind-limb ischemia-reperfusion damage were the first to investigate muscle regeneration, as opposed to behavior of a cell line. Both are providing impetus for more *in vivo* experimentation.

EVs derived from differentiating PHMs can also confer a myogenic profile (eg. increased expression of MyoD and increased cell fusion) to human adipose-derived stem cells [82]. These researchers found a reduced fibrotic area *in vivo*, following injection of EVs into lacerated mouse skeletal muscle. Although the research described so far is very illuminating, it was limited to animal models.

3.3.2 EVs and exercise

Very few studies have investigated the nature of EVs in the context of exercise: only 3 studies can be reported here.

Following an acute bout of aerobic exercise (50 minutes at 60-70 % of VO_2peak), microvesicles were isolated from plasma derived from 8 ml blood samples [83]. These authors did not identify EVs using any of the markers discussed above, but relied solely on size calibrated flow cytometry isolating particles < 1 μm in diameter (i.e. within the microvesicle range) that were also positively stained for one or more of the endothelial proteins CD34 and/or CD62E. Using only these cell surface markers it was not possible for the authors to make any pronouncements on the effects of exercise on microvesicle or exosome release. However, their objective was to investigate the endothelial marker enrichment and they found gender-based differences: $CD34^+$

EVs and $CD62E^+$ EVs were elevated to different extents immediately post-exercise when comparing males and females, respectively. A generalised conclusion from this study could be that exercise may affect vesicle composition.

Fruhbeis et al [84] showed that the EV number in plasma increases immediately after an acute bout of aerobic exercise (incremental cycling or running to fatigue), returning to baseline numbers at 90 mins post-exercise. Although 12 subjects were recruited for this study, all of whom exercised at least 3 hours per week, 8 performed the cycling test and only 4 performed the running test. Although not explained, one might presume this was due to their habitual exercise choice. In keeping with the evolution of EV analysis techniques in the cell studies, these authors used NTA technology along with western blotting to characterise EVs isolated by ultracentrifugation. However, in-depth EV cargo analysis was not done in this study. It should also be noted that comprehensive analysis was not done for all subjects i.e. for each exercise discipline two subjects' EVs were analysed using NTA, whereas 6 (cycling) and 4 (running) were analysed only by western blotting. Nonetheless, this was the first study to report increased EV release up to 2-fold immediately post-exercise. Blotting for TSG101 did not reveal a similar increase in band density to what may have been expected based on the NTA results. Taken together these data suggest that exercise is a significant stimulus for EV release, but more studies are required to better identify EVs in this context convincingly.

Taking a different approach, *Guescini et al* related resting EVs to aerobic fitness rather than investigating an acute effect of exercise on EV mobilization [34]. EVs were identified as originating from muscle by positivity for SGCA. Furthermore, they showed that $SGCA^+$ immuno-captured EVs were enriched in miR-206, which as mentioned earlier is a myomiR and hence confirmed muscle as their tissue of origin. They also showed that baseline plasma levels of myomiR-1, myomiR-133b and myomiR-206 in EVs were statistically significantly and positively correlated to VO_2 max, a measure of aerobic fitness. To our knowledge, this is the only study that has measured myomiRs packaged in EVs from human subjects, although several reviews now promote the notion of EV and myomiRs as circulating communicators of SkM [85] [86] [87].

3.3.3 EVs and myomiRs

Skeletal muscle exhibits a distinct enrichment in microRNAs that suggests tissue-critical roles. The term "myomiR" has been used to describe the family of miRs with key roles in both cardiac and skeletal muscle regulation [88]. A good example of this is shown in myostatin null mice, who show an increased expression of all canonical myomiRs in skeletal muscle lysates [89]. Four archetypal myomiRs, working in close conjunction with the MRFs, have been shown to be of particular importance; miR-1, 206, 133a and 133b [90]. MyomiRs are detected in muscle lysates, as well as in blood, and their expression is altered during different physiological states [91] [92]. The potential of myomiRs as a key component of SkM understanding is highlighted by the surge in research trying to detect circulating myomiR profiles that could serve as biomarkers for myopathies [93] [94] [95].

In addition to being possible biomarkers, the functional effects of the myomiRs that form part of EV cargo must be considered. miR-1 and miR-206 are involved in promoting myoblast differentiation, whereas miR-133a and miR-133b are seemingly involved in promoting proliferation [90]. However, the exact roles of miR-133a and miR-133b remain unclear. Of the myomiRs, miR-1 expression is often reported to exhibit the largest changes in response to stimuli [96] [97]. In as early as 2005, the importance of miR-1 was revealed in its ability to produce a myogenic profile when transfected into HELA cells [72].

Further than just enrichment, some miRs are considered tissue-specific. These are defined as existing in twenty-fold greater abundance in a particular tissue when compared to their average in other tissues [98]. Of the myomiRs, miR-206 is the only established SkM-specific miR [98].Other myomiRs occur in cardiac and smooth muscle cells/tissue. Tissue-specificity suggests a tissue-specific function. In miR-206 knockout studies, no overt change in myoblast phenotype was noted *in vitro* [99]. However, a delay in the regenerative response to cardiotoxin-induced SkM injury was seen *in vivo* [21]. Interestingly, MyoD and myostatin are both transcriptional activators of miR-206 [100] [101]. Much like the MRF protein, MyoD, miR-206 is considered pivotal in SkM, and its expression is increased throughout myoblast differentiation [102] [103]. Indeed, miR-206 is known

to repress the expression of Paired box transcription factor 7 (Pax7), a protein that aids SC quiescence, thereby allowing SC activation and differentiation [104].

Another important miR in myoblast regulation is miR-31. Although not classified as a myomiR, miR-31 has been shown to bind Myf5 at the transcript level, contributing to the maintenance of SC quiescence [17]. Interestingly, miR-31 is also known to target dystrophin mRNA, and its expression is greatly elevated in muscle biopsies from Duchenne muscular dystrophy patients [105].

In the context of exercise, *Banzet et al* shown that myomiRs are not significantly affected by concentrically-biased exercise. In contrast, miR-1, 133a and 133b are elevated within 6 hr following eccentrically-biased exercise [91]. Recently, *Coenen-Stass et al* found no changes in circulating myomiR levels in mice for the subsequent 7 days following a 20 min aerobic exercise regimen [106]. *In vitro*, however, they noted a large and consistent increase in miR-133a and miR-206 in the media of PHM switched to differentiation for nine days, with no change in miR-31 noted. Importantly, both these studies considered total circulating miRs in their analyses, rather than miRs specifically packaged in EVs. It is clear that more detailed information is needed on myomiRs to fully elucidate their roles in SkM.

Aims and objectives

Following review of the literature, the hypothesis formulated for this thesis was that:

"Exercise-induced muscle damage causes substantial changes in circulating extracellular vesicles"

To address this hypothesis this thesis aimed:

"To determine whether circulating exosome size, number and cargo is altered in response to exercise-induced muscle damage from an acute bout of eccentrically-biased exercise."

Specific Objectives:

1. To use a combination of two eccentrically-biased exercise protocols to produce EIMD.
2. To quantify the number and sizes of exosomes pre and post EIMD.
3. To analyse selected protein content of exosomes pre and post EIMD using two techniques:
    a. Tetraspanin CD9 immunogold labeling with TEM visualisation.
    b. Global qualitative assessment of protein with Coomassie gel staining.
4. To analyse the expression of select miRs in exosomes, in response to an acute bout of EIMD:
    a. myomiR-1, 133a and 133b.
    b. SkM-specific miR-206.
    c. miR-31 (known to be involved in regulation of the MRF, Myf5).

Chapter 4: Materials and methods

4.1 Ethical considerations

This study was approved by Stellenbosch University's Health Research Ethics Committee (Study reference: N15/08/075), and was carried out in accordance with the guidelines of the South African Medical Research Council.

4.2 Participants

n = 9 healthy, untrained males between the age of 18 and 30 volunteered for this study. Exclusion criteria for participants included; regular exercise exceeding 2 bouts per week, participation in professional sports, or the use of anti-inflammatory medication within 3 months preceding the study. Furthermore, participants were required to be in good health (i.e. with no chronic illness), and were not to have participated in any strenuous exercise in the 3 weeks preceding the study.

4.3 Eccentric exercise regimen

Each participant performed an acute bout of eccentric exercise that consisted of plyometric jumping (PMJ) and downhill running (DHR). The protocol was modified from two similar protocols previously used in our lab [13] [23]. The combined exercise protocol was chosen due to prior results indicating that PMJ targets almost exclusively the fast twitch fibres, whereas running recruits both fibre types [13] [23]. Hence, it was hypothesised that combining the two protocols would resultant in more diffuse muscle damage. Both exercise types use the large quadriceps muscles and their antagonists, possibly maximising the potential for EV release from SkM.

Briefly, fasted participants arrived at the exercise lab in the morning, and were guided through a 5 min warm-up focused to the quadricep muscles. Following this, all participants were required to complete 10 sets of 10 plyometric jumps at 90 % of their maximum achievable jump height, with a 1 min interval between sets. Upon completion of the PMJ regimen, a 5 min rest

period was given before commencement of the DHR regimen. Briefly, participants were required to perform 5 sets of 5 min bouts of downhill running at 10 km/ hr, at a 10 % decline (Figure 4.1), and a 2 min standing interval between sets.

Figure 4.1. Image of participant performing the downhill running regimen. The rear end of the treadmill was elevated to achieve an angle of 10 % decline.

4.4 Perceived muscle soreness and blood sampling

Following the DHR regimen, whole blood was drawn from the antecubital vein before exercise (i.e. baseline), and at 2 hr and 24 hr post-exercise by a certified phlebotomist. On completion of the exercise regimen, participants were given a standard meal replacement shake and requested not to eat until they returned for the 2 hr blood draw. Participants arrived for the exercise intervention fasted, and the shake was given to standardize a post-exercise meal. Participants were requested to not take part in strenuous activity until they returned the next day for the 24 hr blood draw.

Plasma was isolated from whole blood for subsequent EV isolation. Briefly, whole blood was collected into EDTA-coated tubes and centrifuged at 1200 g for 10 mins at 4° C. Plasma was aliquoted and immediately frozen at - 80° C. Additionally, another aliquot of whole blood was collected into heparin-coated tubes for serum creatine kinase analysis (analysis by PathCare, South Africa). In this analysis, the change in absorption of UV light, caused by a reaction

coupled to NADH production, is read by a microplate reader. At 2, 24 and 48 hr post-exercise, participants gave a rating (out of 10) of their perceived muscle soreness upon walking and with the application of thumb pressure to the quadriceps muscles. A score of 0 signified no pain, with 10 signifying extreme pain.

4.5 EV isolation

EVs were isolated from plasma using qEV size exclusion columns (iZon Science), according to the manufacturer's protocol (Figure 4.2). The specifications of these columns result in a predominantly exosome, rather than microvesicle, isolate. Henceforth, this isolate will be termed exosomes. Briefly, plasma was thawed on ice and centrifuged at 15 000 g for 10 mins to remove cellular debris. The qEV columns were washed with 5 ml of freshly filtered PBS, and the flow rate was determined as a measure of column cleanliness. Subsequently, 1ml of plasma was added to the top of the column (Figure 4.2 blue arrow), and multiple 500 µl fractions of the resultant elution were collected. qEV columns were continuously topped with PBS, as to not allow the filter to run dry. Fractions 7 to 9 were pooled due to their known high vesicle number and purity, along with a reasonably low dilution of the exosomes. Samples were aliquoted and frozen at -80° C. (See Appendix 3 for a comparison of EV isolation techniques)

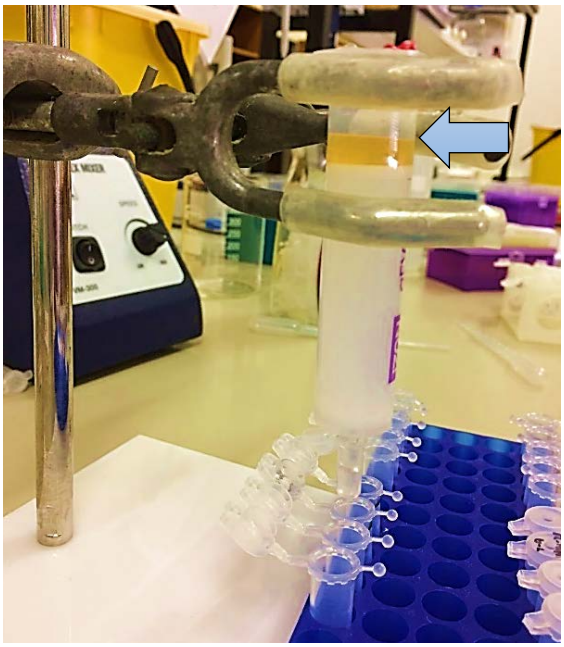

Figure 4.2. Image of exosome isolation process with qEV size exclusion columns (iZon Science). Purified plasma is loaded above the stationery phase (see blue arrow), following which constituents are separated through a Sepharose matrix. 500 µl fractions were collected into Eppendorf tubes, and fractions 7-9 were pooled for downstream exosome analysis.

4.6 Transmission Electron Microscopy

200 mesh, carbon-coated copper TEM grids were glow-discharged, and incubated on 10 µl droplets of sample for 5 mins (Figure 4.3). Grids were then washed with dH_2O and carefully dabbed onto Whatman paper. Following this, grids were incubated on 10 µl of freshly filtered 2 % uranyl acetate (a negative stain) for contrast. For CD9 labelling of isolated exosomes, grids were incubated with mouse, anti-human CD9 primary antibody (1:50, BD Biosciences; 551808) for 30 mins, washed, and subsequently incubated with anti-mouse NanoGold (from here on termed immune-gold) secondary antibody (1:20, Sigma-Aldrich; G7527) before being stained with uranyl acetate. Grids were viewed at 200 kV on a Phillips Tecnai TEM.

Image 4.3. Copper TEM grids are incubated on 10 µl of sample for maximum proximity of grids to exosomes. After each step, grids are incubated on distilled water, and carefully dabbed onto absorbent Whatman paper as a washing step.

4.7 Gel electrophoresis

Samples were run on 1.5 mm SDS-PAGE gels with a 12 % resolving gel. A 10-well comb was used to enable a maximum loading volume of 66 µl. Gels were electrophoresed at 70 V for 2-3 hours and detected using the Bio-Rad ChemiDoc imaging system.

Gels were washed with dH_2O, and incubated with Coomassie brilliant blue dye (Sigma-Aldrich) for 30 mins. Following this, sequential steps of de-staining (30 % Methanol, 10 % Acetic acid and 60 % dH_2O) was done for 5, 30 and 120 mins.

4.8 RNA isolation

Total RNA was isolated from exosomes using the Total Exosome RNA and Protein isolation kit, per the manufacturer's guidelines (ThermoFisher Scientific; 4478545). 600 µl of exosome isolate was mixed with denaturing solution in a 1:1 ratio. RNA was isolated by acid-phenol: chloroform extraction, using an 11 000 g, 15 mins centrifugation for separation. The resultant aqueous phase was removed and diluted 1:1 with 100 % ethanol. 700 µl of the RNA/ Ethanol mix was loaded onto glass fibre filter-containing columns and centrifuged at 11 000 g for 15 sec. The filtrate was discarded and the column was loaded two more times in order to maximise RNA recovery. The RNA-bound column was sequentially washed with two ethanolic solutions of differing concentrations, and eluted with a low ionic-strength buffer. Samples were immediately frozen at -80° C.

4.9 MicroRNA analysis

Reverse transcription and pre-amplification of microRNA was achieved with the TaqMan Advanced miRNA cDNA synthesis kit (ThermoFisher Scientific; A28007). In an initial poly-A tailing reaction, 2 µl of total RNA was added to a poly(A) polymerase mix. Next, the product underwent ligation with an adaptor sequence. The adaptor ligase activity is dependent upon a 5′ phosphate, only present on mature microRNAs. In the reverse transcription reaction, the poly(A) tail is recognised by an oligo-dt primer that aids the action of a universal reverse transcriptase in transcribing the ligated microRNA. Given the low copy numbers of miRs found in biofluids, an extra miR amplification step is added with the use of universal forward and reverse primers that recognise the adaptor sequence.

50 µl of the amplified reverse transcription product was diluted in a 1:10 ratio for subsequent qPCR analysis. 5 µl of this diluted cDNA was loaded into fast optical 96-well plates, and the plates were sealed with optical adhesive film. qPCR analysis was performed in duplicates on a StepOne qPCR thermocycler (Applied Biosystems). TaqMan Advanced miRNA assays; miR-1 (477820_mir), miR-133a (478511_mir), miR-133b (480871_mir), miR-206 (477968_mir) and miR-31 (478015_mir) were used (all obtained from ThermoFisher Scientific). The full names for these miRs are; hsa-miR-1-3p hsa-miR-133a-3p, hsa-miR-133b, hsa-miR-206 and hsa-mir-31-5p, respectively.

Additionally, 1pM of the synthetic C. Elegans oligo, cel-miR-39 (Sequence: UCACCGGGUGUAAAUCAGCUUG), was added to the isolated total RNA. This sequence does not exist in humans and was used as an exogenous control [107]. cel-miR-39 was reverse transcribed and amplified with all samples, and all qPCR reactions were normalised to the resultant cel-miR-39 Ct values. (See Appendix 2 for a more detailed discussion on this microRNA workflow)

4.10 Nanoparticle Tracking Analysis

Vesicle size and number were analysed with nanoparticle tracking analysis (NTA), using the NanoSight NS500 (Malvern Instruments). Analysis was performed at the Council for Scientific

and Industrial Research (CSIR, Pretoria, South Africa). Exosome isolates were diluted in PBS (1:200) for a suitable number of particles per frame, and five 30 second videos were used to determine particle numbers per ml and mean particle diameter. (See Appendix 5 for more information on NTA theory)

4.11 Statistical analysis

All data are represented as mean ± standard error of the mean (SEM). Parametric data were analysed by means of a two-way ANOVA, with a Fisher LSD post-hoc test. A mixed model two-way ANOVA was used for data with unmatched repeated measures. MicroRNA Ct values were normalised to an exogenous control by subtracting the sample from the control value. Graphs were made using version 5 of GraphPad Prism (GraphPad Software inc, USA), and statistical significance was set at a 5 % confidence interval i.e. $p < 0.05$.

Chapter 5: Results

5.1 Participants

9 healthy male participants, between the age of 18 and 25, successfully completed the exercise protocol. Mean participant height and weight was 179 ± 1.86 cm and 76 ± 4 kg, respectively.

5.2 Indirect assessment of muscle damage

5.2.1 Perceived muscle pain (PMP)

Participants were asked to rate their PMP on a scale of 1-10 (1 = no pain, and 10 = extreme pain). Regarding pain in the anterior quadriceps, two indices were measured; PMP upon walking and PMP upon palpation. Ratings were obtained at 2, 24 and 48 hr post-exercise. PMP upon walking was found to be significantly higher at 24 hr ($p < 0.001$) and 48 hr ($p < 0.05$), when compared to 2 hr post-exercise (Figure 5.1.A). A similar pattern was found for PMP upon palpation of the quadriceps, with a significant increase in perceived pain occurring at 24 hr ($p < 0.01$) and 48 hr ($p < 0.05$), when compared to 2 hr post-exercise (Figure 5.1.B). Both measures displayed a plateau between the 24 hr and 48 hr timepoints. The PMP scores observed here are in alignment with the timeframe for DOMS manifestation.

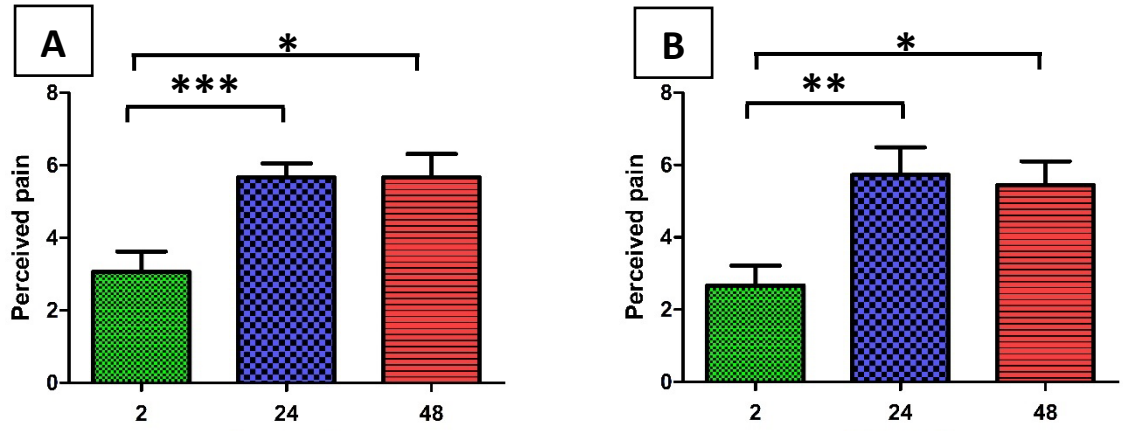

Figure 5.1. Perceived muscle pain of the anterior quadriceps upon walking (A) and palpation (B). A large increase in pain scores is seen for both indices at 24 hr and 48 hr, when compared to 2 hr post-exercise. (Repeated measures ANOVA. Mean ± SEM, *p<0.05, **p<0.01, ***p<0.001. n = 9).

5.2.2 Serum creatine kinase (CK) activity

Serum CK activity, measured in international units/liter (IU/L), is a clinically used indicator of muscle damage. To support the findings obtained from PMP scores, serum CK activity was measured at baseline (BL), and at 2 hr and 24 hr post-exercise (Figure 5.2). When compared to BL, CK activity was significantly elevated at 24 hr post-exercise ($p < 0.001$). A significant difference in CK activity was also observed between 2 hr and 24 hr post-exercise ($p < 0.001$), whereas no change was noted between BL and 2 hr post-exercise. Taken together, PMP and CK analysis confirmed that the exercise intervention had a significant effect on skeletal muscle.

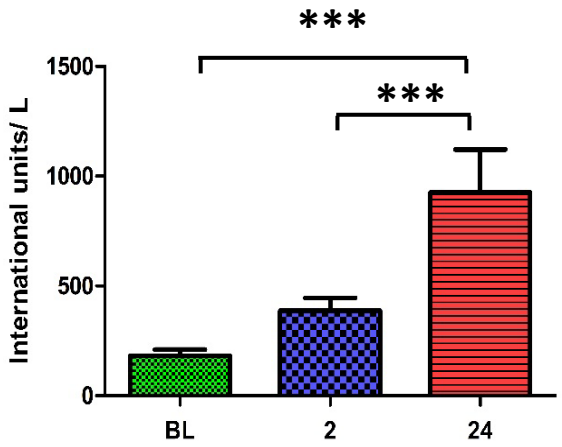

Figure 5.2. Serum creatine kinase activity before and after the exercise intervention. Values are represented in international units (IU) per litre. (Repeated measures ANOVA. Mean ± SEM. ***p<0.001. n = 9).

5.3 Assessment of the EV Isolation method

The qEV size exclusion columns (SEC) utilised in this study have previously been used in the published literature to isolate exosomes from human plasma [108]. To confirm the presence of exosomes in the pooled fractions (fractions 7-9) obtained from plasma pre and post exercise, an aliquot of the isolated fractions was visualised using TEM**.** An abundance of vesicles with the expected diameter and morphology of exosomes were found to be present (Figure 5.3 A-D). The spherical appearance of these vesicles suggests that they were isolated in an intact state, and had not been lysed by the isolation process. As expected, qualitative assessment of the TEM

images suggested that the majority of isolated EVs fell within the exosome size range (30-150 nm), with vesicles in the microvesicle size range (100-1000 nm) appearing less frequently (see Figure 5.3.A arrows pointing to microvesicles). Highly-resolved visualisation of ± 50 nm exosomes was achieved (Figure 4.D).

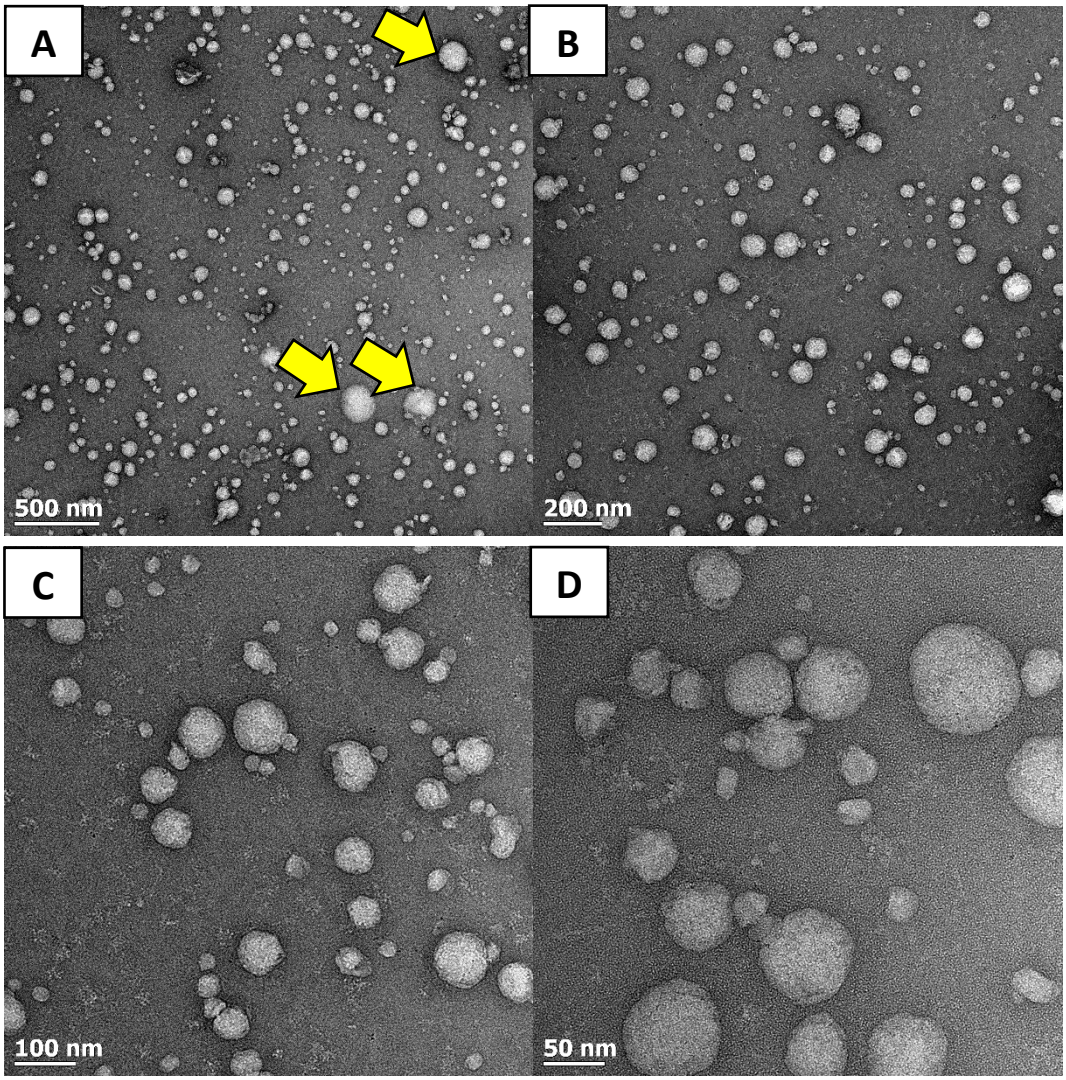

Figure 5.3. TEM images of exosomes at increasing magnifications (A-D). A: a wide-field image revealing the abundance of exosomes. EVs within the exosome size range predominate, with microvesicles appearing less frequently (yellow arrows). B & C: confirmation of intact vesicle, suggesting that they are rendered intact by the isolation process. D: highly resolved images of small exosomes. Blurring of the membrane suggests that this size range is approaching the limit of resolution. (TEM = Transmission electron microscopy).

Immuno-gold labelling of pooled exosome fractions was also visualised with TEM. Mouse, anti-human CD9 primary antibodies, in conjunction with gold-labelled anti-mouse secondary antibodies were used. Sufficient contrast to visualise exosomes and 10 nm gold nanoparticles simultaneously was achieved with high-resolution brightfield imaging (Figure 5.4). Immuno-gold labelling was limited to the exosome membrane as would be expected with labelling of the transmembrane protein, CD9 (Figure 5.4 yellow arrows). CD9 is a widely-used marker of exosomes, and this result therefore further substantiates that the isolation method indeed yielded exosomes of high purity.

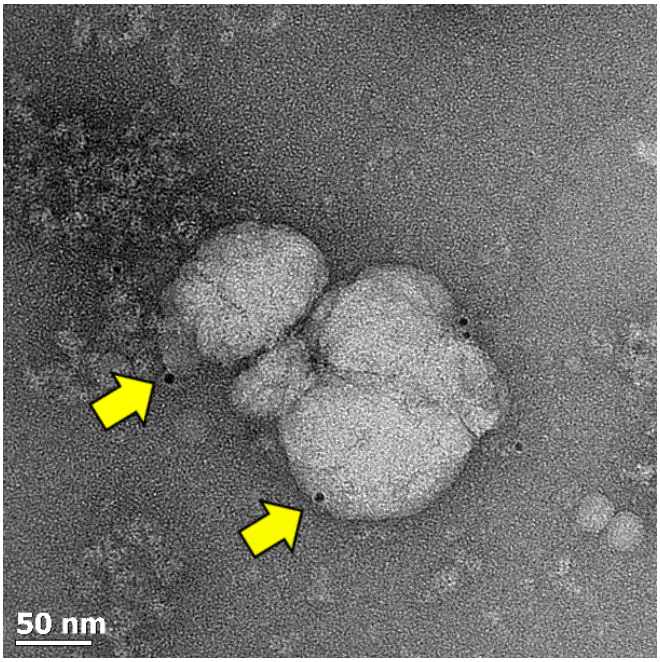

Figure 5.4. Highly-resolved TEM image of immuno-gold labelled exosomes. Clearly visible gold nanoparticles (± 10 nm, yellow arrows) are seen on the membrane. Antibodies against the exosome-enriched transmembrane protein, CD9, were used.

5.4 Quantitative exosome analysis with NTA

To obtain more quantitative data on the numbers and sizes of exosomes obtained using the qEV SEC method, samples were subjected to NTA. The pooled fractions were abundant in vesicles within the exosome size range (i.e. 30-150 nm). An example of this can be seen by the peaks in the representative NTA report graph in Figure 5.5.

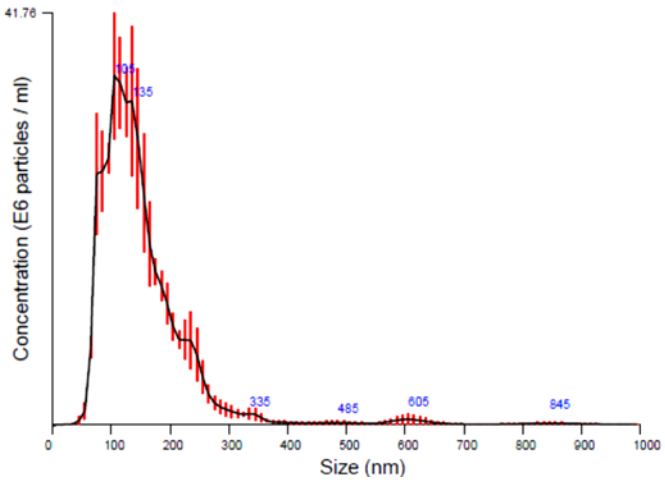

Figure 5.5. Representative graph of particles/ ml vs particle diameter (nm) from a Nanoparticle tracking analysis report. The graph represents the mean of 5 runs from one of the 26 samples measured. Red error bars denote SEM. (Dilution: 1:200).

Statistical analysis of vesicle number and size indicated no significant differences between timepoints. The mean vesicle diameter present in the isolated fractions was 127 ± 15 nm (Figure 5.6.A), while the mean number of vesicles/ml was 9.5 x 10^{10} ± 5.4 x 10^{9} across all timepoints (Figure 5.6.B). The combined results of TEM and NTA, demonstrate that successful isolation of exosomes from human plasma had been achieved, with the exercise intervention having no effect.

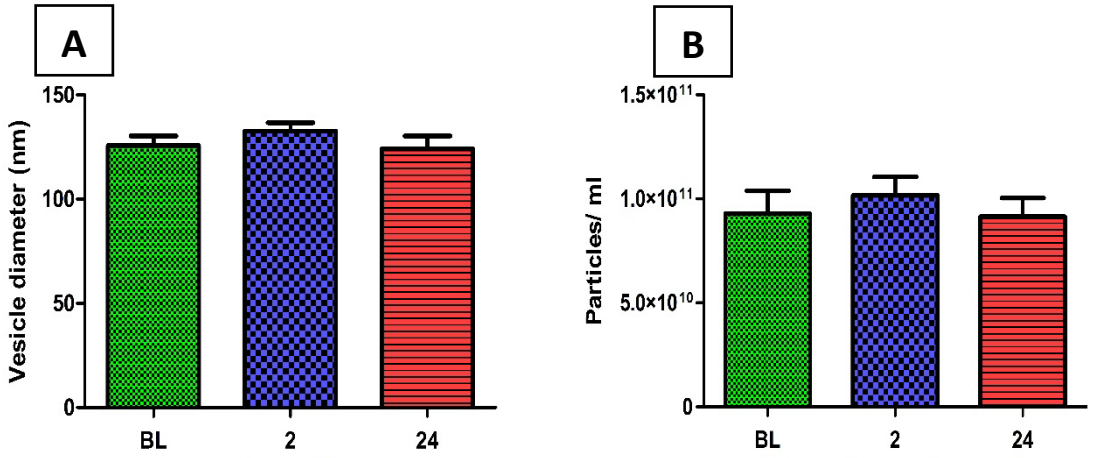

Figure 5.6. Nanoparticle tracking analysis results across all timepoints. No change in vesicle diameters (A) or particles/ ml (B) were noted over time. (ANOVA. Mean ± SEM. n = 9 for BL and 24 hr. n = 8 for 2 hr).

5.5 Protein concentration of exosomes

The next aim was to ascertain whether a difference in protein concentration may be present in isolated EVs pre and post exercise. No significant changes in protein concentration between timepoints were noted (Figure 5.7).

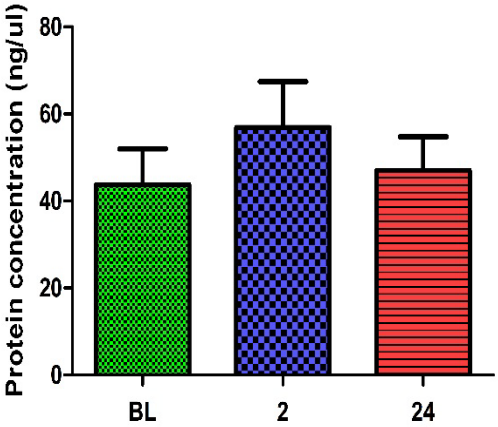

Figure 5.7. Exosome protein concentrations for each timepoint. Protein concentration is represented in ng/ μl. (ANOVA. Mean ± SEM n = 8 for BL, n = 7 for 2 hr and n = 8 for 24 hr).

5.6 Qualitative proteome comparison

A preliminary investigation of whether there may be changes in the types of proteins present in exosomes pre and post exercise was done by visually assessing a Coomassie stain of isolated exosomes loaded onto a 12 % resolving gel (Figure 5.8). Results suggest that there could be a difference in the proteome of exosomes isolated pre and post-exercise, whereby exosomes post-exercise show a greater band intensity at the ± 50-75 kDa range. Additionally, protein bands were more prominent in participant 1 than in participant 2. Notably, also present in exosomes are large proteins that migrate at > 250 kDa.

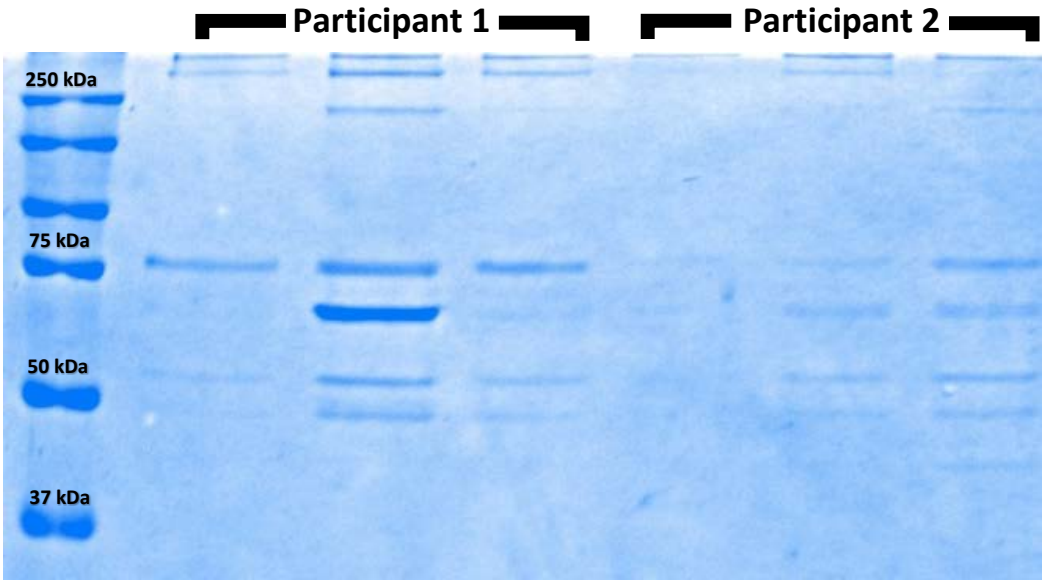

Figure 5.8. Image of Coomassie stained resolving gel. Electrophoresed exosome proteins of all timepoints are displayed for 2 randomly chosen participant (= 6 lanes). Major bands are prevalent at ± 50, 55, 65, 75 and 300 kDa. (Ladder = BioRad Kaleidoscope).

5.7 EV MicroRNA expression

miRs are an important biological cargo of exosomes and may have an important role in SkM regeneration. Based on results in published literature, five miRs were selected for investigation in this study; miR-1, 133a, 133b, 206 and 31. Initial analysis of the miR data demonstrated that expression levels for the SkM-specific, miR-206, were diverse. In one participant, expression was not detectable at any timepoint, while for another expression was detected at all three timepoints. However, most participants exhibited a miR-206 value for at least one timepoint (n = 8). In contrast to miR-206, miR-1 was the most abundantly expressed miR, with strong expression (Ct < 30) detected in all but one of the 26 samples. miR expression was normalised to an exogenous control (cel-miR-39), and expressed as relative expression of their Ct value (i.e. ΔCt). ΔCt was converted to - ΔCt so that statistical analysis and graphs would show the orientation to denote changes in expression (i.e. larger Ct values correspond to lower miR expression. Here, the graphs purely represent expression). Statistical analysis of miR expression levels did not reveal any significant difference between timepoints for miR-1 (Figure 5.9.A), miR-133a (Figure 5.9.B), miR-133b (Figure 5.9.C) or miR-206 (Figure 5.9.D). Expression of miR-

31, however, was found to be significantly lower at 24 hr ($p < 0.05$) post-exercise when compared to BL (Figure 5.9.E).

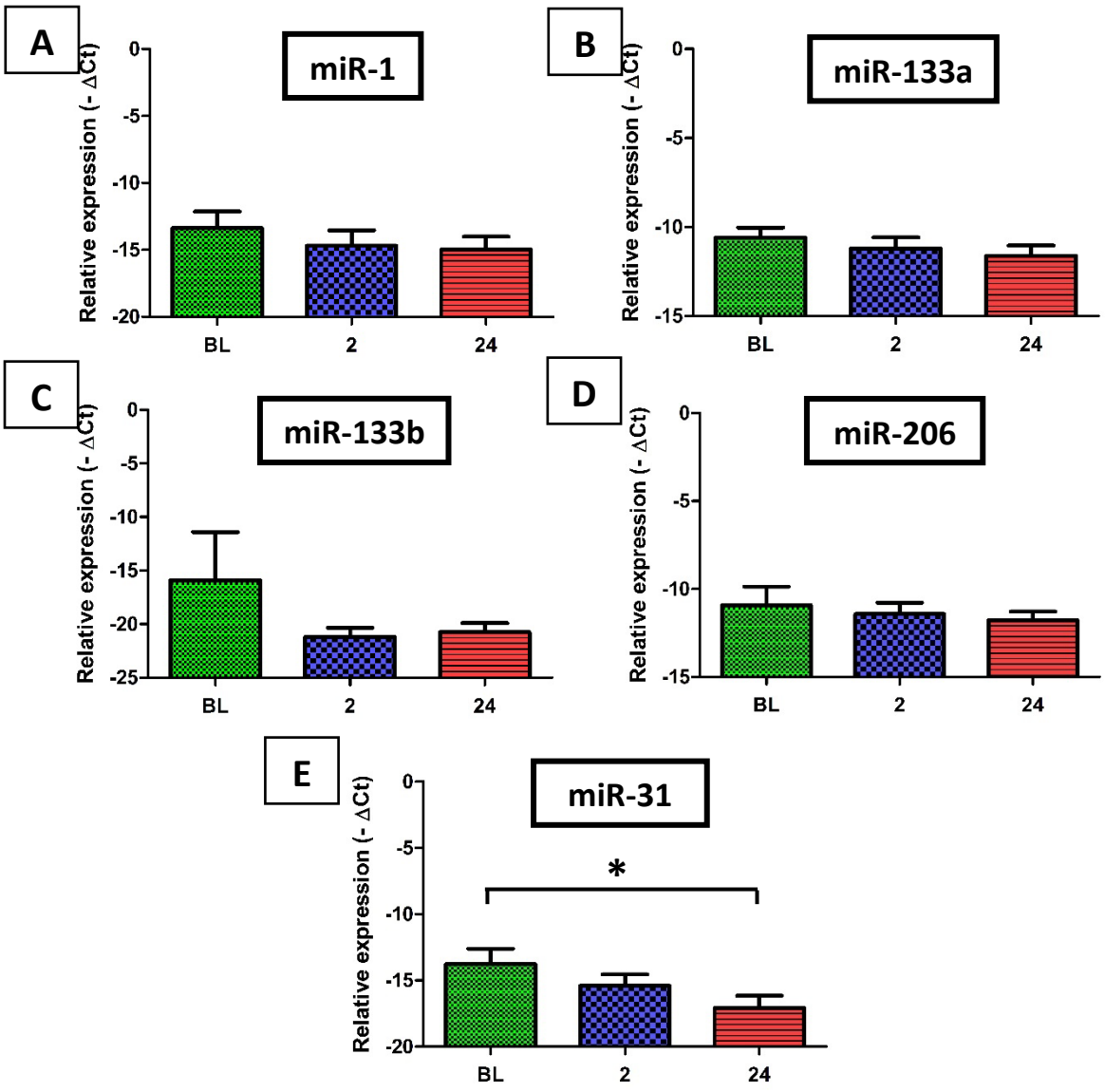

Figure 5.9. Relative expression of five exosome microRNA levels normalised to the exogenous control, cel-miR-39. A-D: relative expression of myomiRs, with no changes noted over time. E: decrease in miR-31 at 24 hr when compared to BL. Data are represented as relative expression, as - ΔCt. (ANOVA. Mean ± SEM. * $p < 0.05$. n = 9 for BL, n = 8 for 2 hr and n = 9 for 24 hr).

5.8 Responders vs non-responders

A disparity in the response of participants to EIMD is a known phenomenon often noted, and referred to in the literature as participants being responders or non-responders [22] [25] [109]. To ascertain whether this phenomenon may be present in our exosome data, a classification system based on vesicle numbers was devised. If a participant had a > 1.5-fold increase in vesicle numbers between baseline and 24 hr post-exercise, they were designated as "responders" (n = 3). In contrast, if they exhibited a decrease in exosome numbers over the same timepoints, they were designated as "non-responder" (n = 6). Due to the small number of participants in the responder group, no statistical analyses were performed to compare the two groups. However, for the non-responder group, a re-analysis of the relative miR expression was performed to see if there was an effect of miR content over time in participants who had not released more exosomes, but could have released exosomes with a different cargo content. A significant change in miR-133a expression was found, whereby it had decreased between BL and 2 hr ($p < 0.05$), as well as between BL and 24 hr ($p < 0.05$) post exercise (Figure 5.10). This miR expression change was not found when all participants were grouped together.

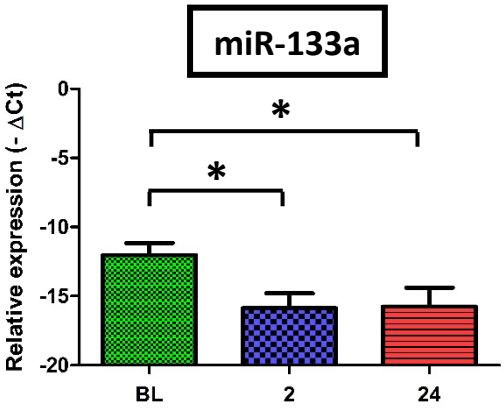

Figure 5.10. Relative expression changes in miR-133a unveiled after grouping non-responders. Data are represented as relative expression, as - ΔCt. (ANOVA. Mean ± SEM. * $p < 0.05$. n = 5).

Chapter 6: Discussion

This thesis aimed to determine whether an acute bout of muscle-damaging exercise would alter the dynamics of circulating exosomes, their protein and selected miR content. It was hypothesised that the *in vivo* model of heavily eccentrically-biased exercise in human volunteers would result in substantial changes in systemic communication via exosomes, with the numbers, sizes and cargo profile of circulating exosomes changing in parallel, and reflecting a skeletal muscle origin.

6.1 Exercise mode

Research on circulating exosome responses to exercise is in its infancy, with only a few studies published that have investigated the effects of incremental exercise to fatigue [84], aerobic exercise lasting 40 mins at 80 % of their VO2max [34] or until a total energy expenditure of 598 kcal [83]. There are a multitude of exercise modes, intensities and durations that could have been chosen for this study. However, there are several reasons that exercise that would inflict muscle damage was used: *in vitro* work has all been done on C2C12s [77 79 80] or PHMs [78 86] cells, these myoblast cells are known to respond to eccentrically-biased exercise modes *in vivo*, including after PMJ [23] and DHR [13 24]. These data, along with the large size of the muscles used during PMJ and DHR, lead us to hypothesise that an eccentrically-biased protocol would likely result in substantial changes in systemic communication *via* exosomes.

Exosomes are known to be enriched in miRs [41]. As mentioned in the introductory section (Chapter 3.3.3), myomiRs (as well as miR-31) work in close conjunction with MRFs [17 89 100 101]. Eccentric exercise is known to cause changes in measures associated with alterations in MRF expression levels [10 13], as well as the expression of myomiRs [91]. Therefore providing further data to substantiate the choice of an eccentrically-biased protocol.

Indirect evidence for EIMD was achieved through the large increase in serum CK activity and PMP following the exercise protocol. A > 5-fold increase in serum CK activity was seen between

BL and 24 hr. Notably, elevation in serum CK activity is the most widely used indirect marker of EIMD [12]. The large elevation in CK activity observed in all participants reinforced confidence that the chosen exercise intervention would have activated muscle regeneration processes. This is substantiated by *van de Vyver et al*, who have shown not only a large peak in CK after an acute bout of DHR at similar timepoints to those used in this study, but also a concomitant increase in SC activation 24 hr post-exercise [13]. Similarly, *Macaluso et al* have shown disruption of sarcomere ultrastructure following an acute bout of PMJ [23]. From these data, it was concluded that the model of EIMD used in this study was sufficient to serve as a putative model for inducing significant changes in the profile of circulating exosomes.

6.2 Qualitative and quantitative analysis of exosomes

The merit of exosome isolation through SEC was qualitatively shown by the abundance of exosomes per field of view in TEM images. As mentioned before, the qEV SEC method predominantly isolates EVs within the exosome size range. High-resolution TEM visualisation showed that exosomes were rendered intact. Interestingly, the samples did not present with the "typical" cup-shaped morphology noted by some research groups [31 57 110]. It seems that this cup-shape noted by some other research groups is likely due to desiccation of the sample, or by harsh chemical fixation [111], whereas fresh vesicles were fixed using the negative stain (i.e. uranyl acetate) as the fixative in this study. A more comprehensive qualitative analysis of exosomes was achieved through visualisation of the exosome-enriched transmembrane protein, CD9, by immuno-gold labelling. Regarding the proximity of gold nanoparticles to the exosome membrane, we could conclude that $CD9^+$ exosomes were indeed present.

The number of exosomes derived from participants' plasma (± 9 x 10^{10} vesicles/ml) supports the notion that these vesicles exist as significant mediators of systemic communication. Recently, using isolation and analysis techniques similar to those used here, *Gamez-Velero et al* determined the mean exosome concentration in plasma from four subjects to be 1.9 x 10^{10} vesicles/ml [112]. Here we show, using a sample size of 9, a significantly greater mean concentration of 9 x 10^{10} vesicles/ml. The infancy of EV biology has left a lack of consensus on nomenclature, isolation

techniques and interpretation of results, making comparisons between studies difficult. Differences in EV results across studies are often attributed to differences in methodology and sample, but this is further confounded by the common variation noted in human studies. However, mean exosome diameters differed by just 11 nm between the aforementioned and current study (mean diameters of 116 nm and 127 nm, respectively), suggesting the similarity of exosome isolation and analysis. Large variability in circulating exosome numbers between human participants was seen in both studies. When considering the deviation from the mean at the different timepoints in the current study (SEM. BL: 1.0×10^{10}, 2 hr: 8.8×10^{9}, 24 hr: 8.9×10^{9} vesicles/ml), although also influenced by the relatively small sample size, the inherent variation in human measures (such as those seen in CK responses to eccentric exercise) was apparent in exosome quantification. One might conclude that variability increases when humans are subjected to a physiologically taxing intervention.

Recently, *Gamez-Velero et al* were unable to detect exosome protein concentrations using standard techniques (Nanodrop and BCA). Similarly, the protein concentrations of SEC-derived samples were also below the detection limit of standard quantification techniques. However, here the exosome protein concentration was successfully quantified using a microBCA kit. The low protein concentrations were also visible on Coomassie-stained gels. Approximately 200 ng of exosome protein was the maximum that could be accommodated in each well, far below the ug range at which most western blot experiments are performed. Attempts to concentrate exosome proteins using a 3 kDa spin column were also unsuccessful (see Appendix 4). The low protein concentration, however, is not necessarily indicative of low vesicle numbers, as shown by the NTA results. Expressing exosome concentration as vesicles/ ug protein, suggests that a low protein content per single vesicle was apparent. Interestingly, results obtained from Coomassie stained gels highlighted the presence of proteins (eg. ± 50 and 65 kDa) at post-exercise timepoints that were not visible at BL. Such a finding suggests that while protein concentration of exosomes may not change significantly during the post-EIMD timepoints assessed here, the proteome profile of circulating exosomes may still be altered. However, it is important to note that this particular set of results was obtained from just two participants for a preliminary qualitative view. The future use of more advanced, albeit costly, techniques such as

mass spectrometry will need to be applied in the analysis of exosomes pre and post EIMD in order for such findings to be properly verified.

Recently, *Webber et al* have proposed the representation of exosome concentrations as vesicles per ug of protein [113]. To better determine the purity of exosome isolates, and suggest the potential contamination of unwanted proteins (e.g. from media or serum), they proposed a high purity of exosomes to be > 1 x 10^{10} vesicles per ug protein (derived from serum using ultracentrifugation). With the currently reported analysis of minimally perturbed plasma-derived exosomes using SEC isolation, approximately 2 x 10^{15} vesicles per ug of protein was achieved, suggesting the high purity of the exosome isolate in this study.

6.3 SkM microRNAs are systemically circulated

6.3.1 MyomiRs

The myomiRs, miR-1, 133a, 133b and 206 contents in exosomes were analysed in the current study, but did not show any significant relative changes resulting from EIMD. Recently, *Kramers et al* determined a substantial increase in circulating exosome numbers immediately after aerobic exercise [84]. Within 90 mins, they found that exosome numbers returned to BL levels. Considering this, it is plausible that the 2 hr timepoint selected for the current study may have missed an immediate systemic response. However, one reason for selecting the 2 hour timepoint was that this is a timepoint when the pro-inflammatory response to eccentrically-biased exercise is most evident [24].

Nonetheless, the presence of the skeletal muscle-specific myomiR, miR-206, within circulating exosomes, gives further insight into the role of skeletal muscle as a systemic communicator. This supports the existing knowledge that SkM is very active in the release of cytokines and immune activators, dynamically changing this profile following exercise [114]. It is clear that the understanding of systemic communication with regard to this large tissue will aid in the greater understanding of interleaving physiological processes not only involved in muscle biology.

6.3.2 The miR-31 axis

For this study, miR-31 was selected for investigation due to its known involvement in regulation of the myogenic transcription factor, Myf5, at the transcript level [17]. Myf5 is an important MRF, implicated in the commitment of SC to terminal differentiation, as well as in the maintenance of this progenitor cell's pool size [17]. *Crist et al* have shown that Myf5 protein increases in SCs upon activation, with a concomitant decrease in miR-31 expression [17]. These researchers concluded that Myf5 was "primed" for translation by miR-31 repression at the transcript level. Although not assessed here, the timeline of peak SC activation following an acute bout of muscle-damaging exercise has previously been shown at 24 hr post-exercise in a study using the exercise mode of DHR [13]. The lower miR-31 expression within exosomes in the current study therefore coincides with this peak activation of SC, and one might speculate based on other studies a concomitant increase in Myf5 protein. In support of this "***SC, Myf5, miR-31 axis***", miR-31 has also been shown to be downregulated during myoblast differentiation *in vitro* [115]. Here it was shown the miR-31 component of this axis was released to a lesser extent 24 hr post-EIMD, suggesting downregulation may also occur *in vivo,* at a timepoint when Myf5 mRNA repression is likely to decline.

6.3.3 Responders vs non-responders

In this study we propose a classification of responders to EIMD through participant response to EIMD. As mentioned before, only 3 participants showed an exosome increase > 1.5-fold 24 hr post-exercise. Here we show that when re-analysis of miR data was done on non-responders (n = 6), miR-133a showed a significant decrease in exosomes at 2 hr and 24 hr post-exercise, a finding that was not apparent when all participants were analysed together. These findings suggest that participant response groupings may be an important factor to consider in EV and miR analysis.

6.4 Conclusion

Systemic intercellular communication is not a new concept. A plethora of information on the dynamics of circulating hormones, cytokines and peptides is available for a host of different

states *in vivo*. In contrast, the understanding of exosome dynamics is only just beginning to be unraveled. Due to their recent emergence, small size and limited cargo, exosome analysis lies at the very edge of current technology. The current interpretation of exosome dynamics and profiles will therefore most likely develop slowly with each new study, adding only a few answers whilst raising even more questions to be answered.

Using SEC as an exosome isolation method, along with a simplified protocol for fast exosome visualisation using TEM, and quantification using NTA, this study was the first to probe the effects of eccentrically-biased exercise on exosome dynamics in human subjects. Using the combination of techniques here, it can be concluded that isolation of exosomes was successful based on the expected size range and the intact nature of vesicles visualised. The two main biological findings were a) that circulating exosome numbers differ substantially between human subjects, both prior and after a taxing intervention and b) that a 22 nucleotide microRNA, miR-31, is decreased within exosomes in response to the physiologically intensive, non-invasive perturbation that induced symptoms of exercise-induced muscle damage.

Chapter 7: Limitations and future directions

It is clear from this study that the analysis of human samples can be considerably variable, a point that is emphasised by disparate responses of participants to exercise. As noted in this study and in the literature, EIMD delineates groups of responders and non-responders to muscle damage based on the CK responses [22] [25] [109]. In this study we propose a new grouping system based on changes in exosome numbers, with participants showing > 1.5-fold increase at 24 hr post-exercise being grouped as responders, and those showing a decrease being grouped as non-responders. However, our groupings revealed just 3 participants in the responders group, greatly decreasing statistical power for subsequent exosome miR content comparison. Future studies would benefit from greater participant numbers that would help resolve definitive groupings, and perhaps provide a partial description for the variable responses to EIMD seen in humans.

Briefly mentioned in the introduction section, no single indirect indicator of muscle damage can be taken as an absolute measure. Visualisation of sarcomere damage from muscle biopsies can be used to directly indicate damage, but a combination of strategies is necessary for indirect measures. Muscle biopsies were not taken in this study as the biopsy procedure could potentially cause changes in skeletal muscle exosome release and subsequent analysis of the circulating exosomes. Measurements of force output were not done for this same reason. Here, the use of serum CK activity and PMP could be improved upon with the addition of circulating inflammatory marker analysis (at the minimum, IL-6) and the measurement of isometric force loss, aiding confirmation of EIMD. However, it remains true that muscle damage can only be accurately validated in muscle biopsies themselves.

Although the proximity of immuno-gold to the membrane of exosomes was not present on grids incubated with the immuno-gold conjugated secondary alone, significant non-specific binding to the TEM grid was noted. This non-specific binding was likely due to the high

concentrations of secondary used (i.e. 1 : 50). Nonetheless, further optimization and analysis of exosome immuno-labelling will be required to definitively determine the presence of CD9 on exosome membranes.

In the current investigation, blood draw timepoints were chosen in accordance with known changes in SkM-related events in circulation. The 2 hr post-exercise timepoint was chosen in accordance with peak elevation in the inflammatory cytokine, IL-6, from a similar DHR protocol [24]. Similarly, the 24 hr timepoint was chosen in knowledge that peak satellite cell, as shown by an increase in Pax 7^{+} cells, in muscle biopsies taken after a similar DHR regimen is seen at that timepoint [13]. The study by *Fruhbeis et al* later revealed a large increase in exosome numbers immediately following an acute bout of aerobic exercise [84], a timepoint that was not used in this study. Additionally, *Banzet et al* found an increase in circulating myomiRs at 6 hr after an acute bout of eccentrically-biased exercise. However, EVs were not taken into account with these myomiR changes. Although the two aforementioned studies cannot directly be translated into the context of this study i.e. use of aerobic exercise and non-EV related myomiRs changes, respectively, it is nonetheless important for researchers to consider additional timepoints to more comprehensively determine the dynamics of circulating EVs e.g. BL, immediately post-exercise, and at 1, 2, 6 and 24 hr post-exercise.

As with EVs, research on miRs is also still in its infancy. miR analysis and reporting of miR data lacks consensus regarding representation of data, use of controls (exogenous and endogenous) and quantification. The analysis of miRs in this study was greatly aided by established knowledge on the analysis of larger RNA species in our lab. This study made use of the new TaqMan Advanced workflow (ThermoFisher Scientific) for miR analysis. This workflow was released in 2015, and we are the first to use it in South Africa. Few studies have been published using this workflow, and to our knowledge, none on exosome miRs. This makes comparison of data difficult. Additionally, the use of exogenous controls such as in this study only controls for qPCR variation, and the identification and validation of an endogenous miR control would greatly improve the interpretation of the miR results. However, as opposed to GAPDH which is used as an endogenous control for mRNA qPCR, no appropriate endogenous miR control has

yet been identified. Regardless of the workflow chosen or the control used, it is apparent in the literature that isolation, analysis and representation of miRs is disparate. More stringent guidelines need to be established by the scientific community as the field progresses.

Lastly, although much research is now directed toward the analysis of miR-206 in circulation, quantification is reported as difficult and variable [91]. Indeed, in the current study, just one participant exhibited a miR-206 value at each timepoint, with one participant having no value at any of the timepoints. The tissue-specific nature of this miR undoubtedly holds great potential in unlocking the intricacies of SkM as a systemic communicator, but it appears that even the basics of miR-206 are far from understood, let alone other myomiRs in relation to miR-206 and the effects of physiologically taxing interventions in otherwise healthy individuals. Therefore, in the near future, we propose that studies involving human subjects should include at least > 9 participants.

List of references

1. Sakuma, K., Aoi, W. & Yamaguchi, A. The intriguing regulators of muscle mass in sarcopenia and muscular dystrophy. *Front. Aging Neurosci.* **6,** 1–17 (2014).

2. Scully, R. E. & Hughes, C. W. The pathology of ischemia of skeletal muscle in man. *Am. J. Pathol.* **32,** 805–29 (1955).

3. Marinacci, A. Rand, C. Nerve Lesions in industry. *Calif. Med.* **88,** 33–38 (1958).

4. Jones, E. Musculoskeletal complications of hemophilia. *Calif. Med.* **6,** 37–42 (1957).

5. Scime, A., Caron, A. Z. & Grenier, G. Advances in myogenic cell transplantation and skeletal muscle tissue engineering. *Front. Biosci.* **14,** 3012–3023 (2009).

6. Morgan, D. L. New insights into the behavior of muscle during active lengthening. *Biophys. J.* **57,** 209–221 (1990).

7. Morgan, D. L. & Proske, U. Popping sarcomere hypothesis explains stretch-induced muscle damage. *Clin. Exp. Pharmacol. Physiol.* **31,** 541–545 (2004).

8. Mauro, A. Satellite cell of skeletal muscle fibers. *J. Biophys. Biochem. Cytol.* **9,** 493–495 (1961).

9. Tidball, J. G. & Villalta, S. A. Regulatory interactions between muscle and the immune system during muscle regeneration. *Am J Physiol Regul Integr Comp Physiol* **298,** R1173-87 (2010).

10. Kanda, K. *et al.* Eccentric exercise-induced delayed-onset muscle soreness and changes in markers of muscle damage and inflammation. *Exerc. Immunol. Rev.* **19,** 72–85 (2013).

11. Morozov, V. I., Tsyplenkov, P. V., Golberg, N. D. & Kalinski, M. I. The effects of high-intensity exercise on skeletal muscle neutrophil myeloperoxidase in untrained and trained rats. *Eur. J. Appl. Physiol.* **97,** 716–722 (2006).

12. Clarkson, P. M. & Hubal, M. J. Exercise-induced muscle damage in humans. *Am. J. Phys. Med. Rehabil.* **81,** S52–S69 (2002).

13. Van De Vyver, M. & Myburgh, K. H. Cytokine and satellite cell responses to muscle damage: Interpretation and possible confounding factors in human studies. *J. Muscle Res. Cell Motil.* **33,** 177–185 (2012).

14. Zhang, C. *et al.* Interleukin-6/signal transducer and activator of transcription 3 (STAT3) pathway is essential for macrophage infiltration and myoblast proliferation during muscle regeneration. *J. Biol. Chem.* **288,** 1489–1499 (2013).

15. Collins, C. A. *et al.* Stem Cell Function , Self-Renewal , and Behavioral Heterogeneity of Cells from the Adult Muscle Satellite Cell Niche. *Cell* **122,** 289–301 (2005).

16. Weintraub, H. *et al.* Activation of muscle-specific genes in pigment, nerve, fat, liver, and fibroblast cell lines by forced expression of MyoD. *Proc. Natl. Acad. Sci. U. S. A.* **86,** 5434–8 (1989).

17. Crist, C. G., Montarras, D. & Buckingham, M. Muscle satellite cells are primed for myogenesis but maintain quiescence with sequestration of Myf5 mRNA targeted by microRNA-31 in mRNP granules. *Cell Stem Cell* **11,** 118–126 (2012).

18. Füchtbauer, E. M. & Westphal, H. MyoD and myogenin are coexpressed in regenerating skeletal muscle of the mouse. *Dev. Dyn.* **193,** 34–39 (1992).

19. Kassar-Duchossoy, L. *et al.* Mrf4 determines skeletal muscle identity in Myf5:Myod double-mutant mice. *Nature* **431,** 466–471 (2004).

20. Dobek, G. L., Fulkerson, N. D., Nicholas, J. & Schneider, B. S. P. Mouse model of muscle crush injury of the legs. *Comp. Med.* **63,** 227–232 (2013).

21. Liu, N. *et al.* MicroRNA-206 promotes skeletal muscle regeneration and delays progression of Duchenne muscular dystrophy in mice. *J. Clin. Invest.* **122,** 2054–2065 (2012).

22. Hubal, M. J., Rubinstein, S. R. & Clarkson, P. M. Mechanisms of variability in strength loss after muscle-lengthening actions. *Med. Sci. Sports Exerc.* **39,** 461–468 (2007).

23. Macaluso, F., Isaacs, a W., Di Felice, V. & Myburgh, K. H. Acute change of titin at mid-sarcomere remains despite 8 wk of plyometric training. *J. Appl. Physiol.* **116,** 1512–9 (2014).

24. van de Vyver, M. & Myburgh, K. H. Variable inflammation and intramuscular STAT3 phosphorylation and myeloperoxidase levels after downhill running. *Scand. J. Med. Sci. Sport.* **24,** e360–e371 (2014).

25. Totsuka, M., Nakaji, S., Suzuki, K., Sugawara, K. & Sato, K. Break point of serum creatine kinase release after endurance exercise. *J. Appl. Physiol.* **93,** 1280–1286 (2002).

26. Nieman, D. C. *et al.* Cytokine changes after a marathon race. *J Appl Physiol* **91,** 109–114 (2001).

27. Smith, Lucille L. McKune, Andrew. Semple, Stuart. Sibanda, Emmanuel. Steel, Helen. Anderson, R. Changes in serum cytokines after repeated bouts of downhill running. *Appl. Physiol. Nutr. Metab.* **32,** 233–240 (2007).

28. Clarkson, P. M. & Sayers, S. P. Etiology of exercise-induced muscle damage. *Canadian Journal Applied Physiology* **24,** 234–248 (1999).

29. Rebalka, I. A. & Hawke, T. J. Potential biomarkers of skeletal muscle damage. *Biomark. Med.* **8,** 375–8 (2014).

30. Yáñez-Mó, M. *et al.* Biological properties of extracellular vesicles and their physiological functions. *J. Extracell. vesicles* **4,** 27066 (2015).

31. Yuana, Y. *et al.* Handling and storage of human body fluids for analysis of extracellular vesicles. *J. Extracell. vesicles* **4,** 29260 (2015).

32. Skotland, T. *et al.* Molecular lipid species in urinary exosomes as potential prostate cancer biomarkers. *Eur. J. Cancer* **70,** 122–132 (2017).

33. Melo, S. a. *et al.* Glypican-1 identifies cancer exosomes and detects early pancreatic cancer. *Nature* **523,** 177–182 (2015).

34. Guescini, M. *et al.* Muscle Releases Alpha-Sarcoglycan Positive Extracellular Vesicles Carrying miRNAs in the Bloodstream. *PLoS One* **10,** e0125094 (2015).

35. Witwer, K. W. *et al.* Standardization of sample collection, isolation and analysis methods in extracellular vesicle research. *J. Extracell. vesicles* **2,** 1–25 (2013).

36. Chargaff, E. & West, R. The biological significance of the thromboplastic protein of blood. *J. Biol. Chem.* 189–197 (1946).

37. Wolf, P. The nature and significance of platelet products in human plasma. *Br. J. Haematol.* **5,** (1967).

38. Pan, B. T. & Johnstone, R. M. Fate of the transferrin receptor during maturation of sheep reticulocytes in vitro: Selective externalization of the receptor. *Cell* **33,** 967–978 (1983).

39. G Raposo, H W Nijman, W Stoorvogel, R Liejendekker, C V Harding, C J Melief, and H. J. G. B Lymphocytes Secrete Antigen-presentingVesicles. *J. Exp. Med.* **183,** 1161–1172 (1996).

40. Ratajczak, J. *et al.* Embryonic stem cell-derived microvesicles reprogram hematopoietic progenitors: evidence for horizontal transfer of mRNA and protein delivery. *Leukemia* **20,** 847–856 (2006).

41. Valadi, H. Ekstrom, K. Bossios, A. Sjostrand, M. Lee, J. Lotvall, J. Exosome-mediated transfer of mRNAs and microRNAs is a novel mechanism of genetic exchange between cells. *Nat. Cell Biol.* **9,** (2007).

42. Pan, B. T., Teng, K., Wu, C., Adam, M. & Johnstone, R. M. Electron microscopic evidence for externalization of the transferrin receptor in vesicular form in sheep reticulocytes. *J. Cell Biol.* **101,** 942–948 (1985).

43. Colombo, M., Raposo, G. & Théry, C. Biogenesis, Secretion, and Intercellular Interactions of Exosomes and Other Extracellular Vesicles. *Annu. Rev. Cell Dev. Biol* **30,** 255–89 (2014).

44. Mayers, J. R. *et al.* ESCRT-0 assembles as a heterotetrameric complex on membranes and binds multiple ubiquitinylated cargoes simultaneously. *J. Biol. Chem.* **286,** 9636–9645 (2011).

45. Stuffers, S., Sem Wegner, C., Stenmark, H. & Brech, A. Multivesicular endosome biogenesis in the absence of ESCRTs. *Traffic* **10,** 925–937 (2009).

46. Theos, A. C. *et al.* A novel pathway for sorting to intralumenal vesicles of multivesicular endosomes involved in organelle morphogenesis. *Dev Cell* **10,** 343–354 (2007).

47. Kaushik, Susmita. Cuervo, A. Chaperone-Mediated Autophagy. *Methods Mol. Biol.* **445,** 1–9 (2008).

48. Wubbolts, R. *et al.* Proteomic and biochemical analyses of human B cell-derived exosomes: Potential implications for their function and multivesicular body formation. *J. Biol. Chem.* **278,** 10963–10972 (2003).

49. Sahu, R. *et al.* Microautophagy of Cytosolic Proteins by Late Endosomes. *Dev. Cell* **20,** 131–139 (2011).

50. Rink, J., Ghigo, E., Kalaidzidis, Y. & Zerial, M. Rab conversion as a mechanism of progression from early to late endosomes. *Cell* **122,** 735–749 (2005).

51. Ostrowski, M. *et al.* Rab27a and Rab27b control different steps of the exosome secretion pathway. *Nat. Cell Biol.* **12,** 19–30 (2010).

52. Möbius, W. *et al.* Recycling compartments and the internal vesicles of multivesicular bodies harbor most of the cholesterol found in the endocytic pathway. *Traffic* **4,** 222–231 (2003).

53. Hess, C. Sadallah, S. Hefti, A. Landmann, R. Schifferli, J.-A. Ectosomes Released by Human Neutrophils ar Specialized Functional Units. *J. Immunol.* **163,** 4564–4573 (1999).

54. Goldie, B. J. *et al.* Activity-associated miRNA are packaged in Map1b-enriched exosomes released from depolarized neurons. *Nucleic Acids Res.* **42,** 9195–9208 (2014).

55. Bianco, F. *et al.* Astrocyte-Derived ATP Induces Vesicle Shedding and IL-1 Release from Microglia. *J. Immunol.* **174,** 7268–7277 (2005).

56. Mulcahy, L. A., Pink, R. C. & Carter, D. R. F. Routes and mechanisms of extracellular vesicle uptake. *J. Extracell. vesicles* **3,** 1–14 (2014).

57. Morelli, A. E. *et al.* Endocytosis, intracellular sorting, and processing of exosomes by dendritic cells. *Blood* **104,** 3257–3266 (2004).

58. Chen, C. *et al.* Imaging and Intracellular Tracking of Cancer Derived Exosomes Using Single Molecule Localization Based Super Resolution Microscope. *ACS Appl. Mater. Interfaces* (2016). doi:10.1021/acsami.6b09442

59. Doherty, G. J. & McMahon, H. T. Mechanisms of endocytosis. *Annu. Rev. Biochem.* **78,** 857–902 (2009).

60. Barrès, C. *et al.* Galectin-5 is bound onto the surface of rat reticulocyte exosomes and modulates vesicle uptake by macrophages. *Blood* **115,** 696–705 (2010).

61. Svensson, K. J. *et al.* Exosome uptake depends on ERK1/2-heat shock protein 27 signaling and lipid raft-mediated endocytosis negatively regulated by caveolin-1. *J. Biol. Chem.* **288,** 17713–17724 (2013).

62. Denzer, K. *et al.* Follicular dendritic cells carry MHC class II-expressing microvesicles at their surface. *J. Immunol.* **165,** 1259–1265 (2000).

63. Alvarez-Erviti, Lydia. Seow, Yiqi. Yin, HaiFang. Betts, Corinne. Lakhal, Sumira. Wood, M. Delivery of siRNA to the mouse brain by systemic injection of targeted exosomes. *Nat. Biotechnol.* **29,** (2010).

64. Record, M., Carayon, K., Poirot, M. & Silvente-Poirot, S. Exosomes as new vesicular lipid transporters involved in cell-cell communication and various pathophysiologies. *Biochim. Biophys. Acta - Mol. Cell Biol. Lipids* **1841,** 108–120 (2014).

65. Brown, D. A. & London, E. Structure and function of sphingolipid- and cholesterol-rich membrane rafts. *J. Biol. Chem.* **275,** 17221–17224 (2000).

66. Pike, L. J. Lipid rafts: bringing order to chaos. *J. Lipid Res.* **44,** 655–67 (2003).

67. Subra, C. *et al.* Exosomes account for vesicle-mediated transcellular transport of activatable phospholipases and prostaglandins. *J. Lipid Res.* **51,** 2105–2120 (2010).

68. Hildonen, S. *et al.* Isolation and mass spectrometry analysis of urinary extraexosomal proteins. *Sci. Rep.* **6,** 36331 (2016).

69. de Menezes-Neto, A. *et al.* Size-exclusion chromatography as a stand-alone methodology identifies novel markers in mass spectrometry analyses of plasma-derived vesicles from healthy individuals. *J. Extracell. vesicles* **4,** 27378 (2015).

70. Lötvall, J. *et al.* Minimal experimental requirements for definition of extracellular vesicles and their functions: a position statement from the International Society for Extracellular Vesicles. *J. Extracell. vesicles* **3,** 26913 (2014).

71. Lunavat, T. R. *et al.* Small RNA deep sequencing discriminates subsets of extracellular vesicles released by melanoma cells - evidence of unique microRNA cargos. *RNA Biol.* **6286,** 00–00 (2015).

72. Lim, L. P. *et al.* Microarray analysis shows that some microRNAs downregulate large numbers of target mRNAs. *Nature* **433,** 769–73 (2005).

73. Ekström, K. *et al.* Monocyte Exosomes Stimulate the Osteogenic Gene Expression of Mesenchymal Stem Cells. *PLoS One* **8,** 2–8 (2013).

74. Sahoo, S. *et al.* Exosomes from Human CD34+ Stem Cells mediate their pro-angiogenic paracrine activity. *Circ. Res.* **109,** 724–728 (2011).

75. Hu, G. *et al.* Exosomes secreted by human-induced pluripotent stem cell-derived mesenchymal stem cells attenuate limb ischemia by promoting angiogenesis in mice. *Stem Cell Res. Ther.* **6,** 10 (2015).

76. Ostenfeld, M. S. *et al.* miRNA profiling of circulating EpCAM + extracellular vesicles: promising biomarkers of colorectal cancer. *J. Extracell. Vesicles* **5,** 31488 (2016).

77. Guescini, M. *et al.* C2C12 myoblasts release micro-vesicles containing mtDNA and proteins involved in signal transduction. *Exp. Cell Res.* **316,** 1977–1984 (2010).

78. Le Bihan, M. C. *et al.* In-depth analysis of the secretome identifies three major independent secretory pathways in differentiating human myoblasts. *J. Proteomics* **77,** 344–356 (2012).

79. Forterre, A. *et al.* Proteomic analysis of C2C12 myoblast and myotube exosome-like vesicles: A new paradigm for myoblast-myotube cross talk? *PLoS One* **9,** (2014).

80. Madison, R. D., McGee, C., Rawson, R. & Robinson, G. a. Extracellular vesicles from a muscle cell line (C2C12) enhance cell survival and neurite outgrowth of a motor neuron cell line (NSC-34). *J. Extracell. vesicles* **3,** 1–9 (2014).

81. Nakamura, Y. *et al.* Mesenchymal-stem-cell-derived exosomes accelerate skeletal muscle regeneration. *FEBS Lett.* **589,** 1257–1265 (2015).

82. Choi, J. S. *et al.* Exosomes from differentiating human skeletal muscle cells trigger myogenesis of stem cells and provide biochemical cues for skeletal muscle regeneration. *J. Control. Release* **222,** 107–115 (2016).

83. Lansford, K. A. *et al.* Effect of acute exercise on circulating angiogenic cell and microparticle populations. *Exp. Physiol.* **101,** 155–67 (2016).

84. Kramers, E.-M. Physical exercise induces rapid release of small extracellular vesicles into the circulation. *J. Extracell. Vesicles* **1,** 1–11 (2015).

85. Quattrocelli, M. & Sampaolesi, M. The mesmiRizing complexity of microRNAs for striated muscle tissue engineering. *Adv. Drug Deliv. Rev.* **88,** 37–52 (2015).

86. Aswad, H., Jalabert, A. & Rome, S. Depleting extracellular vesicles from fetal bovine serum alters proliferation and differentiation of skeletal muscle cells in vitro. *BMC Biotechnol.* **16,** 32 (2016).

87. Aoi, W. Frontier impact of microRNAs in skeletal muscle research: A future perspective. *Front. Physiol.* **6,** 1–5 (2015).

88. Mccarthy, J. J. MicroRNA-206: the skeletal muscle-specific myomiR. *Biochim Biophys Acta* **1779,** 682–691 (2008).

89. Rachagani, S., Cheng, Y. & Reecy, J. M. Myostatin genotype regulates muscle-specific miRNA expression in mouse pectoralis muscle. *BMC Res. Notes* **3,** 297 (2010).

90. Mitchelson, K. R. & Qin, W.-Y. Roles of the canonical myomiRs miR-1, -133 and -206 in cell development and disease. *World J. Biol. Chem.* **6,** 162–208 (2015).

91. Banzet, S. *et al.* Changes in circulating microRNAs levels with exercise modality. *J. Appl. Physiol.* **115,** 1237–44 (2013).

92. Baggish, A. L. *et al.* Dynamic regulation of circulating microRNA during acute exhaustive exercise and sustained aerobic exercise training. *J Physiol* **589,** 3983–3994 (2011).

93. Li, X. *et al.* Circulating Muscle-specific miRNAs in Duchenne Muscular Dystrophy Patients. *Mol. Ther. Nucleic Acids* **3,** e177 (2014).

94. Cacchiarelli, D. *et al.* miR-31 modulates dystrophin expression: new implications for Duchenne muscular dystrophy therapy. *EMBO Rep.* **12,** 136–141 (2011).

95. Matsuzaka, Y. *et al.* Three novel serum biomarkers, miR-1, miR-133a, and miR-206 for Limb-girdle muscular dystrophy, facioscapulohumeral muscular dystrophy, and Becker muscular dystrophy. *Environ. Health Prev. Med.* **19,** 452–458 (2014).

96. Drummond, M. J., McCarthy, J. J., Fry, C. S., Esser, K. A. & Rasmussen, B. B. Aging differentially affects human skeletal muscle microRNA expression at rest and after an anabolic stimulus of resistance exercise and essential amino acids. *Am. J. Physiol. Endocrinol. Metab.* **295,** E1333-1340 (2008).

97. McCarthy, J. J. The MyomiR network in skeletal muscle plasticity. *Exerc Sport Sci Rev* **39,** 150–154 (2011).

98. Lee, E. J. *et al.* Systematic evaluation of microRNA processing patterns in tissues, cell lines, and tumors. *RNA* **14,** 35–42 (2008).

99. Williams, A. H. *et al.* MicroRNA-206 Delays ALS Progression and Promotes Regeneration of Neuromuscular Synapses in Mice. *Science (80-.).* **326,** 1549–1554 (2009).

100. Rosenberg, M. I., Georges, S. A., Asawachaicharn, A., Analau, E. & Tapscott, S. J. MyoD inhibits Fstl1 and Utrn expression by inducing transcription of miR-206. *J. Cell Biol.* **175,** 77–85 (2006).

101. Rao, P. K., Kumar, R. M., Farkhondeh, M., Baskerville, S. & Lodish, H. F. Myogenic factors that regulate expression of muscle-specific microRNAs. *Proc. Natl. Acad. Sci. U. S. A.* **103,** 8721–6 (2006).

102. Ma, G. *et al.* MiR-206, a key modulator of skeletal muscle development and disease. *Int. J. Biol. Sci.* **11,** 345–352 (2015).

103. Hak, K. K., Yong, S. L., Sivaprasad, U., Malhotra, A. & Dutta, A. Muscle-specific microRNA miR-206 promotes muscle differentiation. *J. Cell Biol.* **174,** 677–687 (2006).

104. Dey, B. K., Gagan, J. & Dutta, A. miR-206 and -486 induce myoblast differentiation by downregulating Pax7. *Mol. Cell. Biol.* **31,** 203–14 (2011).

105. Greco, S. *et al.* Common micro-RNA signature in skeletal muscle damage and regeneration induced by Duchenne muscular dystrophy and acute ischemia. *FASEB J.* **23,** 3335–3346 (2009).

106. Coenen-Stass, A. M. L. *et al.* Selective release of muscle-specific, extracellular microRNAs during myogenic differentiation. *Hum. Mol. Genet.* **0,** ddw237 (2016).

107. Roberts, T. C., Coenen-Stass, A. M. L. & Wood, M. J. A. Assessment of RT-qPCR normalization strategies for accurate quantification of extracellular microRNAs in murine Serum. *PLoS One* **9,** (2014).

108. Lobb, R. J. *et al.* Optimized exosome isolation protocol for cell culture supernatant and human plasma. *J. Extracell. Vesicles* **1,** 1–11 (2015).

109. Smith, L. L. *et al.* The impact of a repeated bout of eccentric exercise on muscular strength, muscle soreness and creatine kinase. *Br. J. Sports Med.* **28,** 267–271 (1994).

110. Chairoungdua, A., Smith, D. L., Pochard, P., Hull, M. & Caplan, M. J. Exosome release of B-catenin: A novel mechanism that antagonizes Wnt signaling. *J. Cell Biol.* **190,** 1079–1091 (2010).

111. Raposo, G. & Stoorvogel, W. Extracellular vesicles: Exosomes, microvesicles, and friends. *J. Cell Biol.* **200,** 373–383 (2013).

112. Gámez-Valero, A. *et al.* Size-Exclusion Chromatography-based isolation minimally alters Extracellular Vesicles' characteristics compared to precipitating agents. *Sci. Rep.* **6,** 33641 (2016).

113. Webber, J. & Clayton, A. How pure are your vesicles? *J. Extracell. vesicles* **2,** 1–6 (2013).

114. Pratesi, A., Tarantini, F. & Di Bari, M. Skeletal muscle: An endocrine organ. *Clin. Cases Miner. Bone Metab.* **10,** 11–14 (2013).

115. Dmitriev, P. *et al.* Simultaneous miRNA and mRNA transcriptome profiling of human myoblasts reveals a novel set of myogenic differentiation-associated miRNAs and their target genes. *BMC Genomics* **14,** 265 (2013).

116. Ratajczak, M. Z. & Ratajczak, J. Horizontal transfer of RNA and proteins between cells by extracellular microvesicles: 14 years later. *Clin. Transl. Med.* **5,** 7 (2016).

117. McCarthy, J. J. microRNA and skeletal muscle function: novel potential roles in exercise, diseases, and aging. *Front. Physiol.* **5,** (2014).

118. Lee, E. J. *et al.* Systematic evaluation of microRNA processing patterns in tissues, cell lines, and tumors. *RNA* **14,** 35–42 (2007).

119. McCarthy, J. J., Esser, K. a & Andrade, F. H. MicroRNA-206 is overexpressed in the diaphragm but not the hindlimb muscle of mdx mouse. *Am. J. Physiol. Cell Physiol.* **293,** C451–C457 (2007).

120. Andreu, Z. *et al.* Comparative analysis of EV isolation procedures for miRNAs detection in serum samples. *J. Extracell. Vesicles* **1,** 1–10 (2016).

121. Baranyai, T. *et al.* Isolation of exosomes from blood plasma: Qualitative and quantitative comparison of ultracentrifugation and size exclusion chromatography methods. *PLoS One* **10,** 1–13 (2015).

122. Crossland, R. E., Norden, J., Bibby, L. A., Davis, J. & Dickinson, A. M. *Evaluation of optimal extracellular vesicle small RNA isolation and qRT-PCR normalisation for serum and urine*. *Journal of Immunological Methods* **429,** (Elsevier B.V., 2016).

123. Gardiner, C. *et al.* Techniques used for the isolation and characterization of extracellular vesicles: results of a worldwide survey ´. *J. Extracell. Vesicles* 1–6 (2016). doi:10.3402/jev.v5.32945

124. Van Deun, J. *et al.* The impact of disparate isolation methods for extracellular vesicles on downstream RNA profiling. *J. Extracell. vesicles* **3,** 1–14 (2014).

Appendix 1: microRNA biogenesis, nomenclature & function

Biogenesis

microRNAs (miRs) are either encoded in their own loci in intergenic regions, or from within the introns of other genes [98]. RNA polymerase 2 is an important enzyme that transcribes these loci into RNA transcripts, which immediately fold back on each other to form primary miRs. Cleavage by the enzymes drosha and DGCR8 (DiGeorge syndrome critical unit 8) inside the nucleus results in a 60-70 base pair stem-loop structure, termed precursor miR. This precursor is exported out of the nucleus and cleaved into two ± 22 nucleotide mature miR transcripts (from here on referred to as miRs) by the enzyme dicer. One mature miR is then selectively incorporated into a conglomeration of proteins known as an RNA-induced silencing complexes (RISC), whilst the other is tagged for degradation. RISC proteins facilitate miRs in their repression on mRNA [98].

Nomenclature

miRs are named according to their position on their stem loop precursor; either at the 5p or 3p end (i.e. miR-133a-3p vs miR-133a-5p). Due to poorly understood mechanisms, one of these transcripts is often expressed at a lower level (designated by a *), and it is even possible that one of the transcripts may not be present at any level whatsoever. However, it is important to note that an "unseen" mature miR could be due to our lack of a unified miR understanding, or from imperfect measurement techniques. Furthermore, it is conceivable that these miRs* are fast acting, or only present in certain species. Many miRs can be categorised into families with similar structure and, seemingly, function – serving as a guideline for the mapping of miR activities. Fairly regularly, two miRs from completely different chromosomes can result in sequences that differ by just one nucleotide. These almost identical miRs are denoted with the suffix a or b (i.e. miR-133a vs miR-133b). Similarly, and perhaps most astonishingly, is that miRs

can result in the exact same, indistinguishable sequence despite having originated from separate chromosomes. Furthermore, these two transcripts can be processed from different areas of their stem loop precursors. Although this phenomenon may demonstrate some redundancy, it is interesting to consider that two identical miRs have converged from distinct evolutionary pathways. These identical miRs are labelled with the suffix 1 or 2 (i.e. miR-1-1 vs miR-1-2).

Function

In humans, miRs exert their effects through the transient repression of mRNA translation. They do this by incomplete/ "uncomplimentary" binding, and it is currently thought that the miR seed sequence (approximately 6-8 nts at the 5' end) is of most importance in recognizing mRNAs with some specificity [115]. On the other hand, most plant miRs bind with complete complementarity, and seemingly always result in mRNA degradation. Human miRs therefore have the unique ability to target multiple mRNA transcripts, and consequently, predictive tools regularly establish approximately 300 proposed targets per miR. It is now well known that one mRNA can be targeted by more than one miR, and it is possible for one miR to bind one mRNA at multiple sites. This convolution of information makes prediction of functional outcomes, or the establishment of definitive miR roles, challenging, and therefore miRs can only truly be analysed through gene expression and chromatin-immunoprecipitation studies for now.

Circulating-miRs

Due to blood containing an abundance of RNases, it is easy to accept that RNA is somehow protected within circulation (i.e. within EVs). This knowledge is attractive to many different researchers, such as those looking at; biomarkers for disease, inter-organ communication, regeneration, normal physiology, and even therapeutics. Particular interest lies within the ability to capture actively secreted genetic material, which could potentially provide a novel level of interpretation in physiology. The emerging field of this type of cellular communication has been termed "horizontal gene transfer" [116].

The known existence of miRs within EVs, and the understanding of their known regulatory effects has greatly propagated their interest. There are now over 2500 human miRs identified as per miRBase v.20. (January 2015), whereas most of them are ubiquitously expressed, only a few are tissue specific or enriched [117] [118]. miRs that are tissue-specific are defined as those 20-fold more prevalent in that particular tissue [118]. Muscle-specific miRs are termed myomiRs, and only seven have been identified to date [119]. Five are present in both cardiac and skeletal muscle, whereas each muscle type has only one that is specific. miR-206 is the skeletal muscle-specific miR, and its identification within EVs therefore gives researchers the opportunity to identify circulating EV cargo released from skeletal muscle explicitly.

Appendix 2: microRNA workflow discussed

The TaqMan Advanced microRNA workflow (ThermoFisher Scientific) is optimised for the analysis of multiple mature miRs of limited quantity or in a dilute isolate. The use of this workflow is therefore well suited to the analysis of miRs from biofluids, such as human plasma.

Total RNA isolation

The Total Exosome RNA and protein isolation kit makes use of acid-phenol:chloroform extraction with separation through centrifugation, to delineate proteins and lipids (in the organic phase) from nucleotides (in the aqueous phase). The use of acidic phenol allows for RNA to exclusively occupy the aqueous phase, pulling DNA into the organic phase. The acidic nature of the solution causes the more negatively charged DNA strands to be preferentially neutralized, and hence, more readily precipitated.

The resulting RNA-containing aqueous phase is then loaded onto a glass-fibre filter column. The negatively charged (i.e. due to prevalent phosphate groups) RNA strands, is immobilized on positively charged glass-fibre filters by brief centrifugation at high speeds (i.e. 10 000 g). Small RNAs can be enriched through a second isolation step, making use of a change in the proportion of reagents (i.e. salts and ethanol). RNA is then eluted through the columns using a low ionic strength buffer (i.e. nuclease-free water).

Reverse transcription

The TaqMan Advanced miR cDNA Synthesis kit uses poly(A) tailing, adaptor ligation, reverse transcription and amplification to achieve sufficient cDNA for subsequent qPCR.

The first step of the cDNA synthesis involves the addition of multiple Adenosine nucleotides to the 3′ end of all RNA in the sample, using a poly(A) polymerase (Figure A.1.A). Ligases then add a synthetic adaptor sequence to the 5′ end of RNAs that contain a phosphate group at this

site (Figure A.1.B). In this way, only mature microRNAs are selected. Precursor miRNAs have a 2 nucleotide overhang on the 3′ end, cloaking their 5′ phosphate. This new nucleotide construct is then reverse transcribed by a universal reverse transcriptase and forward and reverse primer recognising the poly(A) tail and adaptor sequence of the construct (Figure A.1.C). This new construct is now "tagged" on both the 3′ and 5′ ends and can be amplified prior to qPCR with universal forward and revers primers (Figure A.1.D).

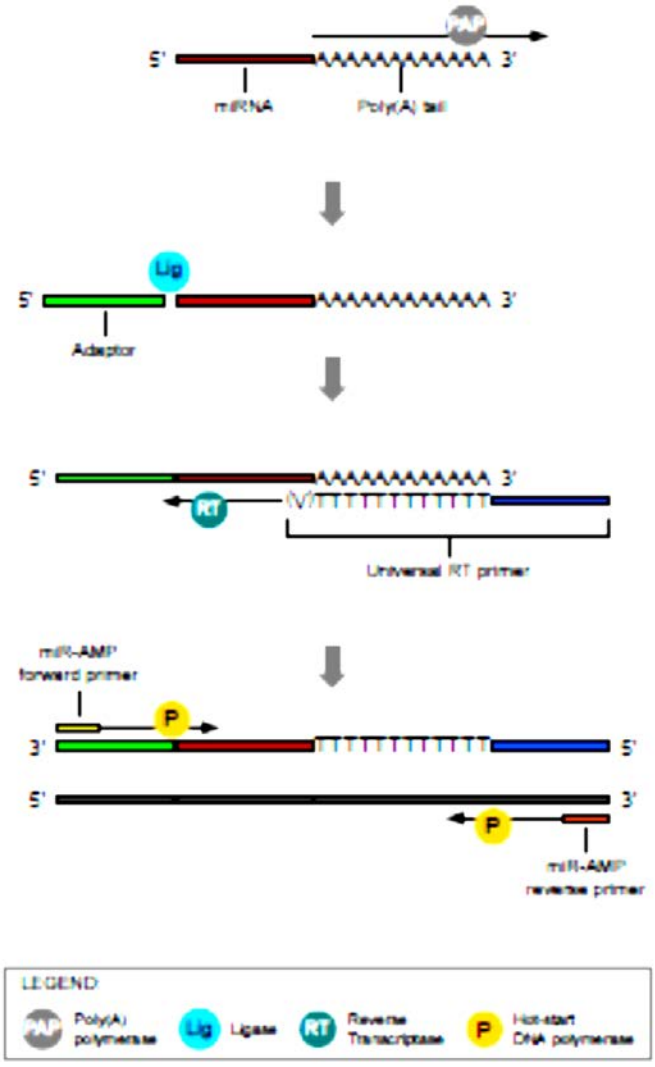

Figure A2. Schematic showing phases of microRNA preparation for subsequent reverse transcription. A: poly (A) tailing of sample microRNA. B: ligation of adaptor sequence. C: conversion of construct into a complimentary sequence. D: amplification of construct with universal primers. Image taken from TaqMan Advanced miR assay user guide (ThermoFisher Scientific).

Quantitative Polymerase Chain Reactions

Quantitative polymerase chain reactions on the resultant cDNA are achieved through the use of specific TaqMan Advanced miR probe. The specificity of TaqMan probes avoids potential primer dimers and non-specific binding sometimes experienced with the use of SYBR green. TaqMan Advanced miR assays are available for all mature human miRs mentioned in version 21 of miRBase. These primers are made up of; a complimentary nucleotide sequence to a specific miR target, a fluorescent reporter dye (i.e. FAM), a non-fluorescent quencher (NFQ) and a minor groove binder (MGB). Presently, TaqMan Advanced primers only contain the blue reporter dye, FAM, at their 5′ end, preventing multiplexed analysis. The 3′ quencher molecule's proximity to the fluorescent dye allows for the absorption of excited electrons, and thus inhibits the release of fluorescence. Therefore, it is only possible to detect fluorescence after Taq polymerases has cleaved the reporter dye and the quencher from the probe. Their loss of proximity means that fluorescence can now be emitted, and is the reason for TaqMan probe's specificity. In addition, the 3′ end makes use of a minor groove binder (MGB) which increases the melting temperature, which can be used to analyse the specificity of primer binding through melting curve analysis.

Appendix 3: A brief comparison of EV isolation techniques

The substantial diversity of EV isolation techniques apparent in the published literature, makes the comparison of data between labs and studies difficult. A consensus on the best, or most suitable isolation method is not yet agreed upon. An absolute method may not be possible, as many research teams have shown that downstream applications vary considerably depending on the method of iolation [120] [112] [121] [122]. A brief overview of the advantages and disadvantages of the different EV isolation methods is show in Table A3. Isolation methods that often appear in the literature can be broadly grouped into; differential centrifugation, density gradients, chemical precipitation, immune-affinity and size exclusion [123].

1. Differential centrifugation

With differential centrifugation, multiple spins are used to rid the sample of cells and debris, after which the sample is ultracentrifuged at high speeds (i.e. > 100 000 g) to pellet the EVs. This is currently the most widely used method and is considered the gold standard in EV isolation. High speed centrifugation was used in the initial EV discoveries [36]. It is now commonplace for researchers to combine ultracentrifugation with sequential steps of filtration (i.e. 0.22-0.45 μm pore size filters) to differentiate between microvesicles and exosomes.

2. Density gradients

More recently, differential centrifugation has been supplemented with sucrose or Iodixanol (OptiPrep) gradients, and sucrose cushions to achieve a more resolved isolate of greater purity. This method makes use of the known EV density range of 1.1 - 1.9 g /ml, resulting in fractionation of the sample per density, rather than size.

	Advantages	Disadvantages
Differential centrifugation	Widely used and therefore translatable. Inexpensive.	Requires large equipment. Time-consuming. Aggregation of EVs.
Density gradients	High specificity. Low contamination. Inexpensive.	Isolation of an undefined EV subpopulation. Difficult to perform. Time-consuming.
Chemical precipitation	Easy to use. Inexpensive.	Non-specific. Potential high contamination
Immune-affinity	High specificity.	Isolation of an undefined EV subpopulation. Dependent on antibody quality. Expensive.
Size exclusion	Short isolation time. Easy to use.	Expensive. Dilutes sample.

Table A3. Comparison of commonly used extracellular vesicle isolation techniques.

3. Chemical precipitation

EV precipitation using precipitating polymers (eg. Polyethylene glycol, ExoQuick, Total Exosome Isolation Reagent) has gained popularity of late. Many researchers have favored this technique due to its low cost and ease of use [120]. The use of precipitating polymers is a well-established technique in the isolation of viral particles. These polymers readily neutralise the charge of biomolecules, thereby decreasing their solubility and causing them to precipitate. However, others have highlighted the potential of this precipitation method to co-isolate a significant amount of contaminating protein due to its non-specific nature [124].

4. Size exclusion

The use of size exclusion columns for the isolation of EVs is an technique that is rapidly increasing in popularity, largely due to its passive isolation of EVs. Most size exclusion techniques make use of Sepharose (GE Healthcare Life Sciences), a bead-based form of the common cross-linking polymer, Agarose. Size exclusion columns (SEC) can also be used to resolve EV fractions derived from other methods. Alternatively, SEC can be used as a standalone technique. Due to the passive nature of SEC EV isolation, the potential for this method to yield intact and functional vesicles is high. The small size of the SEC columns makes

them suitable for use in any lab and does not necessitate access to an expensive ultracentrifuge. Additionally, these columns are known to result in a low amount of contaminant protein co-isolation.

5. Immune-affinity

Immune-capture, or immune-affinity, using conjugated antibodies, is a multidisciplinary technique. This isolation technique includes the use of flow cytometry, magnetic beads or precipitant-conjugated antibodies to capture specific subgroups of EVs in an isolate. Additionally, immune-affinity can be used to remove known contaminants from a sample.

Appendix 4: Concentrating SEC-derived exosome fractions

One drawback of size exclusion columns as an exosome isolation technique is the dilution of sample. SEC uses passive filtration of sample through Sepharose-loaded columns, by adding PBS to follow the sample. The resultant eluent, although resolved, is significantly diluted in PBS. This dilution makes some downstream analyses difficult eg. protein concentration often can't be detected through standard techniques and isolated total RNA cannot be accurately quantified. For these reasons, we attempted to concentrate the SEC-isolated exosome samples.

Pooled fractions (fractions 7-9) were concentrated using 3kDa pore-size, Amicon spin columns (Merck Millipore). These columns were centrifuged at 4 000 g until sufficient sample had eluted through. Approximately 500 µl was loaded per column, and the resultant concentrate was ± 150 µl. Concentrated samples were visualised on TEM grids (Figure A4.1), and displayed obvious signs of exosome aggregation. Exosomes are known to be enriched in cell adhesion molecules and proteins associated with fusion [30]. It is therefore expected that their forced proximity, through concentration, would result in aggregation.

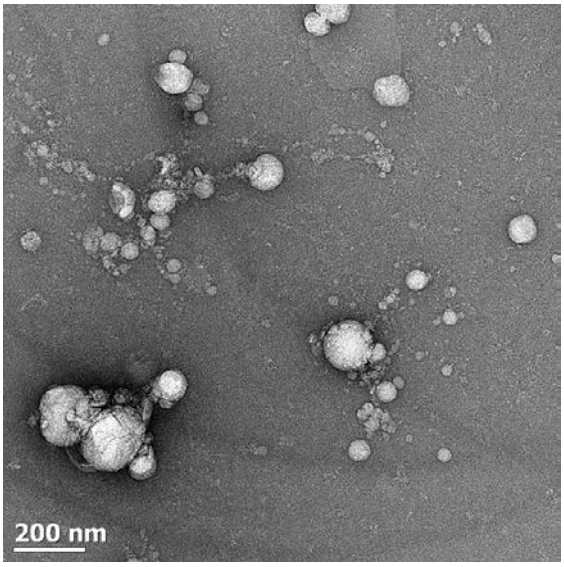

Figure A4.1. TEM image of aggregated exosomes following sample concentration.

We then went on to visualise the concentrated exosome proteins in a Coomassie-stained gel (Figure A4.2). No change in protein content was apparent between normal and concentrated samples across all timepoints, suggesting that the sample concentration was unsuccessful.

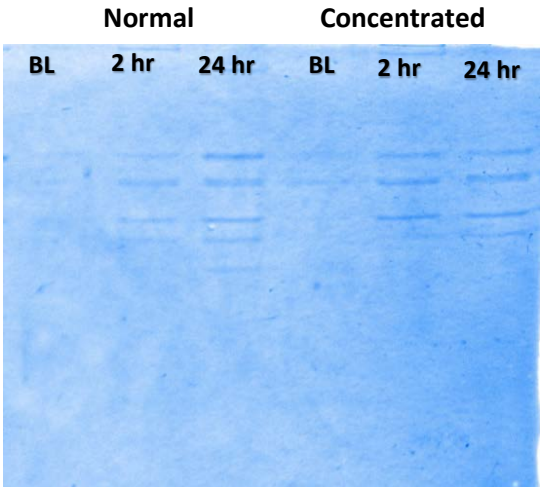

Figure A4.2. Coomassie-stained gel showing normal vs concentrated exosome samples from one participant. Protein from all timepoints was loaded, and no obvious change in protein could be seen.

The difficulty in protein determination, quantification and concentration seen in this study, highlights the need for more advanced proteomic techniques, such as mass spectrometry, to better understand the proteome of SEC-derived exosomes.

Appendix 5: Nanoparticle tracking analysis theory

Nanoparticle tracking analysis (NTA) monitors the inherent motion of microscopic particles in liquid suspension, termed brownion motion. Brownion motion describes the random movement of particles in liquid suspension, resulting from constant interactions with surrounding molecules. Individual particles are tracked based on their dynamic light scattering of a laser beam (Figure A5). Particle size can be determined at just 20 X magnification, by satisfying the criteria of the Stokes-Einstein equation. The equation necessitates that the particles are suspended in a liquid of uniform temperature and viscosity. Particle sizes can then be determined by the speed at which they move, with smaller particles moving faster. Particle numbers (expressed as particles/ml) are extrapolated to the volume of the undiluted, original sample. For sufficient statistical power, vesicle sizes and numbers are determined across 5 x 30 second videos.

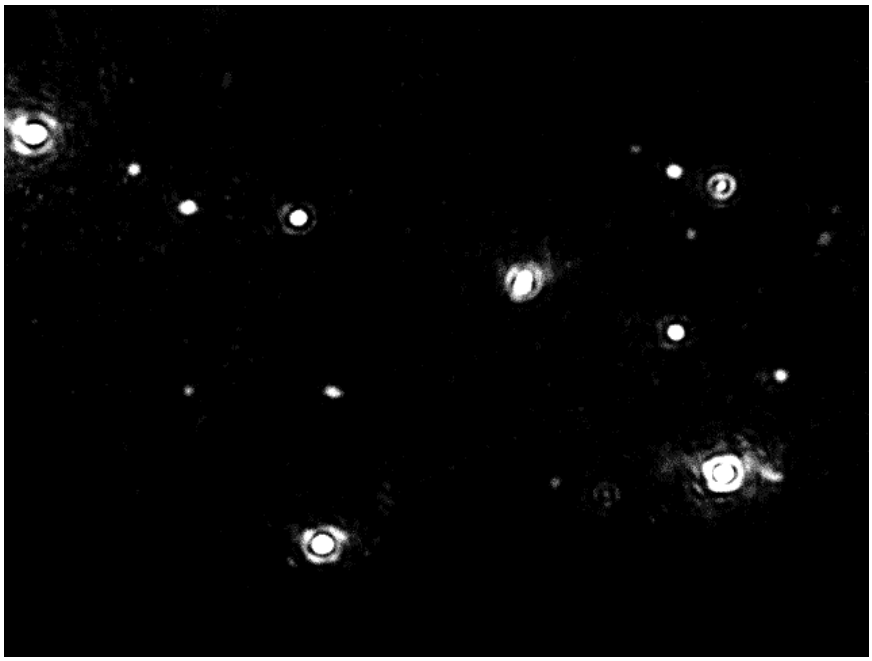

Figure A5. An example of a still image taken from a sample NTA video.